Int.J.Curr.Microbiol.App.Sci (2025) *14*(12): 246-276

International Journal of Current Microbiology and Applied Sciences
ISSN: 2319-7706 **Volume 14 Number 12 (2025)**
Journal homepage: http://www.ijcmas.com

Original Research Article https://doi.org/10.20546/ijcmas.2025.1412.024

Green Synthesis and Characterization of Silver Nanoparticles Using *Phyllanthus pinnatus*: A Study on Antioxidant and Antimicrobial Activities

Shaheen[1] and P. Vijaya[2*]

[1]*Department of Botany, BESTIU - 515231Andhra Pradesh, India*
[2]*Department of Botany, Tara Government College (A), Sanga Reddy - 502001, Telangana, India*

**Corresponding author*

Keywords

Green synthesis, AgNPs, antioxidant, antimicrobial, *Phyllanthus pinnatus* & Phyllanthaceae.

Article Info

Received:
18 October 2025
Accepted:
28 November 2025
Available Online:
10 December 2025

A B S T R A C T

The green synthesis of silver nanoparticles (AgNPs) using various natural resources is one of the emerging fields of green nanotechnology. Silver nanoparticles (AgNPs) were synthesized through an eco-friendly green route using *Phyllanthus pinnatus* leaf extract as a natural reducing and stabilizing agent. The formation of AgNPs was confirmed by a characteristic surface plasmon resonance peak at 445 nm. Structural and morphological analyses using FTIR, XRD, SEM, TEM, and zeta potential revealed predominantly spherical, crystalline nanoparticles with an average size of 10–15 nm and moderate colloidal stability. The biosynthesized AgNPs exhibited concentration-dependent antioxidant activity in DPPH and hydrogen peroxide scavenging assays. Significant antibacterial activity was observed against both Gram-positive and Gram-negative pathogens, with inhibition zones surpassing those of the standard antibiotic ampicillin, particularly against *Streptococcus pneumoniae* and *Pseudomonas aeruginosa*. Moderate antifungal activity was noted at higher concentrations. Overall, the study demonstrates that *P. pinnatus*-mediated AgNPs possess promising antioxidant and broad-spectrum antimicrobial properties, highlighting their potential as sustainable nanomaterials for biomedical and pharmaceutical applications.

Introduction

The concept of "green synthesis" has emerged as a significant paradigm shift in the field of nanoparticle creation (Samuel *et al.,* 2022). During the synthesis of AgNPs, "green synthesis" relates to the utilization of natural resources, including plant extracts, microorganisms, and biomolecules, as stabilizing and reducing agents. This novel methodology adopts the tenets of green chemistry, with the objective of reducing the ecological consequences of synthesis protocols and promoting sustainable methodologies (Gour and Jain, 2019).

This paper delineates nanotechnology. This approach has garnered significant interest in recent years.

Nanoparticles encompass any particles with a diameter ranging from 1 to 100 nm, composed of carbon, metals, metal oxides, or organic compounds (Barhoum *et al.,* 2022). Nanoparticles are different from their larger cousins (Bulk) because they are so small and have a lot of surface area. This makes them better at interacting with other things or staying stable during physical and chemical processes, and it also makes them stronger mechanically, among other things (Khan *et al.,* 2019; Baig *et al.,* 2021; Sabouri *et al.,* 2020). Nanoparticles have diverse shapes and sizes (Yousaf *et al.,* 2022), as well as different diameters. Nanoparticles can be spherical or cylindrical and come in a range of shapes and sizes, from 1 to 100 nanometers. They can be tubular, spiral, flat, or irregular (Kumari and Sarkar, 2021; Saif, 2022). Nanotechnology is advancing swiftly, and numerous rigorous investigations have been undertaken to synthesis nanoparticles with unique attributes regarding cost, completion time, and the specific properties of the produced nanoparticles (Singh, *et al.,* 2002). NPs have been utilized for many things, such as cooking tools, renewable energy, insect control in farming, and a lot in medicine, where they have been used to treat many diseases, move pharmaceuticals, and make materials better (Tulli *et al.,* 2022).

Green synthesis methods utilize natural sources such as plant extracts, microorganisms, and biopolymers as reducing and stabilizing agents for the fabrication of AgNPs. These methods offer several advantages over conventional chemical approaches, including: Environmentally Sustainable; Green synthesis routes minimize the use of toxic chemicals, organic solvents, and energy-intensive processes, thereby reducing the environmental footprint associated with nanoparticle production. Green synthesized AgNPs exhibit enhanced biocompatibility and reduced cytotoxicity compared to chemically synthesized counterparts, making them suitable for biomedical applications such as drug delivery, imaging, and tissue engineering (Le Ouay, and Stellacci, 2015; Sirelkhatim *et al.,* 2015). Natural sources for green synthesis are abundant, renewable, and cost-effective, enabling scalable production of AgNPs with minimal capital investment. Green synthesis methods offer precise control over the size, shape, and surface chemistry of AgNPs through modulation of reaction parameters, enabling customization for specific applications (Hussain, 2022). The utilization of plant extracts and microbial systems for AgNP synthesis capitalizes on the inherent reducing potential of bioactive compounds present in these natural sources, including polyphenols, flavonoids, terpenoids, and proteins. The synthesis mechanism typically involves the reduction of silver ions (Ag^+) to metallic silver (Ag^0) nuclei, followed by their subsequent growth and stabilization into nanoparticles through capping or complexation with biomolecules (Rolim *et al.,* 2019). Moreover, green-synthesized AgNPs exhibit enhanced antimicrobial activity against a broad spectrum of pathogens, making them promising candidates for combating antimicrobial resistance and infectious diseases. Additionally, their catalytic, optical, and electrical properties render them valuable in diverse applications such as catalysis, sensing, electronics, and environmental remediation. This comprehensive review aims to provide a detailed analysis of the green synthesis approaches, characterization techniques, and multifaceted applications of AgNPs (Rai *et al.,* 2016). By elucidating the mechanisms underlying green synthesis routes and exploring the wide-ranging opportunities enabled by green-synthesized AgNPs, this review seeks to contribute to the advancement of sustainable nanotechnology and its integration into various scientific and technological endeavors (Singh *et al.,* 2019).

Silver nanoparticles are some of the most important and prevalent nanoparticles because they have unique qualities like high conductivity and durability. They are also utilized to make therapeutic alloys, to cure burns and infections from wounds, as anti-cancer cells, and to fight viruses, bacteria, and free radicals (Mazhir *et al.,* 2020), and can be utilized in the production of tools that come into contact with food, leading to direct exposure of silver nanoparticles to workers in this sector. This exposure may result in semi-chronic toxic effects and potentially affect the health of the organism, as AgNPs have been shown to precipitate in The kidneys, testicles, lungs, heart, and other organs produce reactive oxygen species in living cells, which can lead to immunological or neurotoxicity(Sabouri *et al.,* 2022), Many studies, on the other hand, have demonstrated that exposure to silver nanoparticles can help treat a number of diseases that are caused by things outside of the body or that last a long time, like diabetes, high blood pressure, or diseases of the immune system (Malhotra and Alghuthaymi, 2021; Von White *et al.,* 2012; El-Refai *et al.,* 2018). There are limited studies that demonstrate the impact of silver nanoparticles on sex cells, as many have indicated. There is a correlation between the dosage administered once and the sanctioned duration of exposure to therapeutic nanoparticles, as well as the health of the sperm (Sabouri *et al.,* 2022). There are other ways to make nanoparticles,

including chemical procedures that employ very harmful and poisonous substances to minimize and stabilize them. These methods are bad for the environment and cost a lot of money and time, and they take a lot of energy. Biological and physical approaches are some of the best ways to make nanoparticles since they are easy, safe, good for the environment, and work well at the same time (Shreyash *et al.,* 2021; Singh *et al.,* 2018). More research and studies are using the biophysical method to make nanoparticles because it is thought to be the best way to use plant-based compounds like polyphenols, flavonoids, anthocyanins, ellagic acid, and other plant materials that can make silver nanoparticles better and less toxic. Metals and salts that are used to make commercial silver nanoparticles (De and Goswami, 2022).

Silver nanoparticles (AgNPs) have emerged as a compelling and highly adaptable category of nanomaterials, garnering considerable interest from the scientific community in several disciplines (Akter *et al.,* 2017). Silver nanoparticles (AgNPs) can be developed using three methods: physical, chemical, and biological. Plants have proven to be promising options for the production of AgNPs because of their superior scalability, nontoxicity, cost-effectiveness, and straightforward synthesis. Furthermore, their biocompatibility and nonpathogenic properties render them suitable for biomedical applications (Xu *et al.,* 2020). Plants have been used as sources of therapeutic compounds for thousands of years, resulting in the extraction of many pharmaceuticals. Substantial research has been conducted to evaluate the biological activity of plant extracts and their constituents.

Plant extracts contain several secondary metabolites such as alkaloids and flavonoids which can function as both capping and reducing agent. Moreover, AgNPs have demonstrated significant potential for oncological research. Their capacity to selectively elicit cytotoxicity in cancer cells while preserving healthy tissue renders them appealing candidates for targeted anticancer therapy (Zielinska *et al.,* 2017). Researchers have thoroughly investigated AgNPs as vehicles for drug delivery, intending to accurately target chemotherapeutic drugs to malignant cells, thus reducing systemic side effects and improving the effectiveness of cancer therapies (Gomes *et al.,* 2021; Xu *et al.,* 2023). The potential of AgNPs to transform cancer therapy is an advancing field of study with significant possibilities for the future of oncology (Jangid *et al.,* 2024).

Silver nanoparticles (AgNPs) are particularly promising in infection control due to their interaction with the mitochondrial respiratory chain, enhancing bioavailability and therapeutic potential against chronic diseases, including cancer (Saratale *et al.,* 2018). Although silver exists in trace amounts in the human body, it plays a role in immune system enhancement (Chernousova and Epple, 2013; Ninan *et al.,* 2020). AgNPs exhibit antibacterial activity against both Gram-positive and Gram-negative bacteria, including silver-resistant *E. coli* (Morones-Ramirez *et al.,* 2013; Ge *et al.,* 2014). Their nanoscale properties enable them to cross biological barriers, improving antimicrobial efficacy (Desai and Taranath, 2013). Due to their high conductivity, chemical stability, and diverse biological activities antimicrobial, anticancer, antidiabetic, and anti-inflammatory AgNPs have garnered extensive interest.

The rich biodiversity of plant sources offers a vast reservoir of bioactive compounds suitable for AgNP synthesis (Eshghi *et al.,* 2018). Various medicinal herbs, fruits, vegetables, and aromatic plants have been explored for their potential in nanoparticle fabrication. Each plant species imparts unique chemical constituents and functional groups to the synthesis process, influencing nanoparticle size, shape, and surface chemistry. Commonly studied plant extracts include Aloe vera, green tea, neem, turmeric, and grapefruit, among others (Selvan *et al.,* 2018).

The plant *Phyllanthus pinnatus* belongs to the family of Phyllanthaceae that consists of approximately 1000 species existing all over the world (Sarin *et al.,* 2014). Up to now, several studies investigated the green synthesis of MNPs by using some species of the genus Phyllanthus. For example, AgNPs were synthesized by using the aqueous plant extract of *Phyllanthus amarus* with spherical shape and size of 24 ± 8 nm. The AgNPs were found to be well dispersed in aqueous medium. Besides, the AgNPs at the concentration range of 12.5–100 lg/mL showed significant in vitro antibacterial activity against different MDR burn isolates of *Pseudomonas aeruginosa* (Singh *et al.,* 2014). In another study, it was reported that leaf mediated synthesized of AgNPs using *Phyllanthus niruri* with the average diameter of 63.45 nm showed antibacterial activity against clinically isolated pathogenic bacteria including *Staphylococcus aureus*, *Escherichia coli*, *Pseudomonous sp*., *Proteus vulgaris*, and *Salmonella typhi* at the concentration of 20 lg/mL (Kathireswari *et al.,* 2014). The current study was aimed to describe a cost-effective

and environ mentally benign technique for green synthesis of AgNPs by using the stem extract of *P. pinnatus* as reducing and stabilizing agent for the first time.

Materials and Methods

Plant materials

The fresh leaves of *Phyllanthus pinnatus* (Wight) G.L. Webster (family Phyllanthaceae), approximately 1 kg in weight, were collected from the Lingala Nallamalla Forest, Achampet Mandal, Nagar Kurnool District, Telangana State, India (16°38′60.00″ N, 80°07′59.88″ E) during August–September 2023.

Authentication of Phyllanthus *pinnatus*

The plant was authenticated by the Department of Botany, Osmania University, Hyderabad, Telangana, and the authenticated specimen was deposited in the Herbarium Hyderbadensis, Department of Botany, Osmania University, Hyderabad, with voucher number OUAS-217.

Drying and Powder Preparation

The collected plant materials were thoroughly washed with double-distilled water to remove dust and debris. The leaves were air-dried at room temperature (25 ± 2 °C) in the shade for approximately three weeks until a constant weight was attained. The dried leaves were then pulverized into a fine powder using a mechanical grinder and stored in airtight containers for further analysis.

Successive extraction using Soxhlet apparatus

Fresh leaves of *Phyllanthus pinnatus* were thoroughly washed under running tap water to remove adhering dust and debris, followed by rinsing with distilled water to eliminate residual impurities. The cleaned leaves were air-dried at room temperature (25 ± 2 °C) and subsequently pulverized into a fine powder using a mechanical grinder. The powdered material was sieved to obtain a uniform particle size and stored in airtight containers until extraction. Sequential extraction was carried out using solvents of increasing polarity petroleum ether, chloroform, ethyl acetate, and methanol employing a Soxhlet apparatus. The extraction was performed for each solvent for approximately 5 hours at temperatures corresponding to their respective boiling points to ensure efficient solvent cycling. The obtained extracts were concentrated using a rotary evaporator and subsequently dried in an oven at 45 °C to remove residual solvent. The dried extracts were stored in desiccators until further use for phytochemical screening (Mahire & Patel, 2020; Khare *et al.,* 2018; Raaman, 2006; Gajula *et al.,* 2022).

Preparation of silver nitrate solution

0.01697 g of $AgNO_3$ was dissolved in 100 mL distilled water to produce 1 mM solution of $AgNO_3$.

Preparation of 0.1 M NaOH solution

0.4 g of NaOH was dissolved per 100 mL of distilled water to prepare 0.1 M NaOH solution and further used to adjust the pH values in different experiments.

Green synthesis of silver nanoparticles

Synthesis of silver nanoparticles using leaf extract

The synthesis of silver nanoparticles (AgNPs) was carried out by mixing 90 mL of double-distilled water containing 1 mM silver nitrate with 10 mL of *Phyllanthus pinnatus* leaf extract in a 1:9 ratio. The reaction mixture was heated to 80 °C using a magnetic stirrer and maintained under continuous stirring at 800 rpm for three hours. A visible color change from yellow to dark brown confirmed the formation of AgNPs. The resulting AgNPs suspension (AgNPs–PPL) was centrifuged at 15,000 rpm for 45 minutes to separate the nanoparticles. The obtained pellet was washed three to four times with deionized water to remove unreacted silver ions and residual plant extract. The purified nanoparticles were then freeze-dried, and the lyophilized AgNPs were stored in a cool, dry, and dark environment. The green-synthesized silver nanoparticles were finally preserved at 4 °C until further characterization and analysis (Pal *et al.,* 2007).

Silver nanoparticles synthesis at varying pH

To enable silver nanoparticle synthesis over a broad pH, range from 3 to 11, solutions were prepared using a fixed volume (15 mL) of leaf extract at a temperature of 80 °C

in both acidic and basic media. The pH adjustment was achieved by slowly adding glacial acetic acid dropwise to lower the pH and sodium hydroxide dropwise to increase the pH.

Characterization of AgNPs -PPL

The synthesized AgNPs of PPL extracts were characterized by UV-Vis- spectroscopy (UV-Vis), Fourier-transform infrared spectroscopy (FTIR), Scanning Electron Microscopy (SEM), X-ray powder diffraction (XRD) and Zeta Potential (ZT).

UV–visible spectroscopy

UV–Visible spectroscopy was employed to monitor and assess the synthesis and stability of metallic nanoparticles, following established protocols for nanoparticle characterization (Astry *et al.,* 1998). Silver nanoparticles typically exhibit a distinct surface plasmon resonance (SPR) band in the UV–Vis spectra, which reflects particle formation and size distribution (Vanden Bout *et al.,* 2011).

In this study, the UV–Visible absorption spectra of the aqueous extract of Phyllanthus pinnatus (PPL) and the synthesized silver nanoparticles were recorded using a Shimadzu UV–Vis spectrophotometer (UV-2450, Japan), with a spectral resolution of 1 nm. The PPL extract served as a natural reducing agent during AgNP synthesis.

All spectroscopic measurements were performed at ambient temperature, utilizing a wavelength range of 300–800 nm, a 1 cm optical path length quartz cuvette, and a scanning rate of 475 nm per minute.

After a 24-hour incubation of silver nitrate (AgNO3) with PPL extract, UV–Visible absorption spectra were measured to confirm nanoparticle formation. A characteristic SPR peak indicated successful silver nanoparticle synthesis. Minor yellow coloration observed in the background was attributed to the use of distilled water (Gong and Krishnan, 2019).

The analysis of the UV–Vis spectra enabled evaluation of the optical characteristics and morphology of AgNPs, providing additional information concerning particle size distribution and confirming the synthesis process (Straková *et al.,* 2020).

Fourier Transforms Infrared Spectroscopy (FTIR)

Fourier transform infrared (FTIR) spectroscopy was employed to identify the functional groups responsible for the reduction and stabilization of AgNPs. Dried PPL leaf powder and AgNPs samples were analyzed using the potassium bromide (KBr) pellet technique in diffuse reflection mode at a resolution of 4 cm^{-1}. Analyses were performed with an FTIR spectrometer (CFRD, Osmania University, Hyderabad, Telangana, India) in the spectral range of 500–4000 cm^{-1}. Both the PPL extract and AgNPs-PPL samples were examined before and after bioreduction (Pakkirisamy *et al.,* 2017; Eid, 2022). The frequency of each vibrational peak depends on the force constant and the reduced mass of the bond, expressed by the following relationship (Ahmed *et al.,* 2021; Al-Otibi *et al.,* 2021)

$\nu = 1/2\pi c \sqrt{(k/\mu)}$
Where ν - is the speed of light,
k- is the force constant
μ- is the reduced mass

Scanning Electron Microscope (SEM)

The structure and size of AgNPs were characterized using a German-made scanning electron microscope (SEM) equipped with EDS, mapping, line analysis, and electron backscatter diffraction (EBSD) capabilities. For SEM analysis, the AgNP sample was first purified by centrifugation at 10,000 rpm for 15 minutes, rinsed with distilled water, and dried at 50 °C. The dried nanoparticles were mounted onto a platinum mesh coated with palladium to enhance conductivity and imaging. The sample was irradiated with a high-energy electron beam in the SEM chamber. Structural morphology and elemental composition were documented using EDS analysis and mapping. Dispersion spectra and imaging were acquired using 250 INCA software settings (Amargeetha *et al.,* 2018).

X-ray Diffraction

The crystal structure and size of silver nanoparticles (AgNPs) were studied using X-ray diffraction (XRD). To prepare for this analysis, 1 mL of colloidal AgNPs was uniformly spread on clean glass plates and oven-dried. This process was repeated two to three times to obtain a thin, consistent film. Glass plates were pre-cleaned with

acetone and ethyl alcohol in an ultrasonic sonicator to remove contaminants prior to nanoparticle deposition. XRD measurements were performed using a Rigaku Ultima IV X-ray Diffractometer (Rigaku, Japan) operated at 40 kV and 30 mA, with Cu-Kα radiation (λ_1 = 1.54056 Å; λ_2 = 1.54439 Å). Thin films of the AgNPs on glass slides were placed in the diffraction arm of the instrument. Diffraction patterns were recorded at 2θ angles ranging from 30° to 80°, and peak intensities were used to calculate crystallite size and analyze phase composition (Kamble *et al.,* 2022). The size of the crystalline AgNPs was calculated using Debye-Scherrer equation, i.e. =

$$D = {}^{K\lambda}/_{\beta\cos\theta}$$

Where, D = Crystalline size of nanoparticles
K = crystalline-shape factor
λ = X-ray wavelength
β = X-ray diffraction broadening, radian
θ = observed peak angle in degree

Zeta potential measurement

The surface electric charge of the synthesized silver nanoparticles (AgNPs) was assessed by measuring their zeta potential, which reflects the electrostatic repulsion ensuring particle stability. Zeta potential measurements were performed using the HAS 300 instrument (Haselmeier, Germany), which operates on the principle of photon correlation spectroscopy (Kibiti and Afolayan 2015). The average zeta potential was recorded over an analysis period of 60 seconds, with measurements conducted on undiluted nanoparticle dispersions.

Antioxidant activity of AgNPs- PPL

(2, 2-Diphenyl-1-picrylhydrazyl) radical scavenging activity assay

The free radical scavenging activity of the AgNPs- PPL silver nanoparticles were analyzed by the 1,1-diphenyl-2-picryl hydrazyl radical (DPPH) method according to Ebrahimzadeh and Bahramian, (2009). This method is based on the reduction of DPPH in methanol solution in the presence of hydrogen donating antioxidant due to the formation of non-radical from DPPH- H, the transformation results in the formation of color change from purple to yellow. In this assay, varying concentrations (10, 25, 50, 75 and 100µg/ml) of compound in 1 ml of methanol solution of DPPH (0.2 mM). There is a need to prepare fresh DPPH 0.2 mM and set OD value to 0.8. If the O.D is less than 0.8 add DPPH or more than 0.8 add methanol. The mixture was thoroughly mixed and incubated for 30 min. The optical density of the solution was then measured at 517 nm using Hitachi 2010 spectrophotometer. Percent inhibition of antioxidant activity was calculated by using the following formula and readings of test sample are compared with the positive control of Ascorbic acid (Vitamin C).

$$\text{DPPH Scavenging activity (\%)} = \left\{ \frac{\text{(Absorbance of control– Absorbance of sample)}}{\text{(Absorbance of control)}} \right\} \times 100$$

Hydrogen peroxide radical scavenging (H_2O_2) Assay

The hydrogen peroxide radical scavenging assay (SA) of AgNPs - PPL was tested by following the procedure suggested by Ruch *et al.,* (1984). Hydrozen peroxide solution 40mM was prepared in phosphate buffer (1M pH 7.4), and the hydrogen peroxide concentration was determined by absorption at 230nm by using a spectrophotometer. PP silver nanoparticles of varying concentration (10-100 µg/ml) in distilled water were added to hydrogen peroxide, and the absorbance at 230nm was determined after 10 min against a blank solution containing phosphate buffer without hydrogen peroxide. The percentage of hydrogen peroxide scavenging was calculated as follows:

% scavenging activity SA = [A control – A sample] / A control x 100

Where A control is the absorbance of the control and A sample is the absorbance of the test sample. The experiments were run in triplicates.

Antibacterial activity (Bhandari *et al.,* 2023; Meri Amerikova *et al.,* 2019)

Bacterial Strains

The bacterial strains Gram positive of *Staphylococcus aureus* (ATCC 25923), *Streptococcus pneumonia* (ATCC 33400), and Gram negative of *Pseudomonas aeruginosa* (ATCC 27853), *E. coli* (ATCC 25922) used in the study were obtained from ATCC.

Media Preparation for Anti-Bacterial Activity

Nutrient Agar Media

Nutrient Agar was obtained from a commercial source and measured 28.0 grams of powder. Then dissolved the powder in 1000 milliliters of distilled water and mixed it thoroughly. The dissolved nutrient agar was sterilized in an autoclave at a temperature of 121^0 C for a duration of 15 minutes. The sterilized media was then utilized for plate production in order to investigate its antibacterial properties.

Nutrient Broth

Nutrient Broth was obtained from a commercial source and measured 1.3 grams of powder. Then dissolved in 100 milliliters of distilled water and mixed it thoroughly. The dissolved nutrient broth was sterilized in an autoclave at a temperature of 121^o C for a duration of 15 minutes. The sterilized broth was then utilized for the militance of the inoculum.

Preparation of stock solution

The stock culture of each organism was prepared by aseptically subculturing each validated test organism onto two nutrient agar slants. One set of slants was maintained as a stock culture, while another set was used as a working culture. The bacterial cultures were kept at a temperature of 4°C in their respective agar slants and utilized as stock cultures. A single glycerol stock was likewise kept at a temperature of 20 °C.

Inoculum preparation

The selected bacterial pathogens were inoculated into nutrient broth and incubated at 37°C for 24 hours and the suspensions were checked to provide approximately 10-5 CFU/ml.

Antibacterial activity of AgNPs- PPL

The antibacterial activity of nanoparticles was assessed using the agar well-diffusion technique. Four concentrations (25, 50, 75, and 100 µl) were tested against bacterial strains including Staphylococcus aureus, Streptococcus pneumoniae, Pseudomonas aeruginosa, and Escherichia coli. The inoculated plates were incubated at 37°C for 18 to 24 hours. After incubation, the diameter of the clear zone indicating bacterial growth inhibition was measured in millimeters. The activity index was calculated, with measurements taken at three fixed orientations per plate, and the average of these measurements was recorded. This method is widely used for evaluating antimicrobial effects by observing the diffusion of the test substance in agar and the resulting growth inhibition around the wells.

Minimum Inhibitory Concentration (MIC) (Sumaiya Naeema Hawar *et al.*, 2023)

Minimum Inhibitory Concentration (MIC), is the lowest concentration of an anti-microbial growth that will inhibit the visible growth of a microorganism after overnight incubation.

Extract Preparation

Extracts were weighed individually 1mg and dissolved in methanol for final stock concentration as 1mg/ml.

As same sample, standard ampicillin also prepared.

Culture Preparation

Loop of culture was inoculated in 3 ml of nutrient broth and incubate 37^0 c for overnight in shaking incubator.

Inoculum Preparation

From overnight grown culture, 20 µl of culture was taken and inoculated in 1.5 ml of nutrient broth and added different concentration of compound and incubated at 37^0 c for overnight in an incubator.

Results and Discussion

After 24 hrs of compound treatment, tubes were observed, and results were noted.

Anti-Fungal Activity (Nair *et al.*, 2014)

Fungal Strains

The fungal strains *Candida albicans* (MTCC 183) and *Aspergillus niger* (MTCC) used in the study was obtained from Microbial type culture collection (MTCC), Institute of Microbial Technology (IMTECH), Chandigarh

Sabouraud Dextrose Agar (SDA)

A commercially purchased Sabouraud dextrose agar was prepared by dissolving and thoroughly mixing 32.5 grams of powder with 500 milliliters of distilled water. Following the dissolution of the SDA and its autoclaving at a temperature of 121° C for a duration of 15 minutes, the SDA was employed to prepare plates for the purpose of investigating its antifungal properties.

Antifungal activity of AgNPs -PPL (Nair *et al.*, 2014)

The well diffusion method was used to test the antifungal activity. Using the spread plate method, the produced SDA culture plates were inoculated with *Aspergillus niger* and *Candida albicans.* For 48 hours, the plates were incubated for fungal activity at 37+2ºC. After 48 hours, the zones surrounding the well on the plates were checked for zone formation, and the zone of inhibition (mm) was calculated.

Observation and Results

Morphological description of *P. pinnatus*

Plant profile

Pullaiah, T & Ali Moulali, D., 1997. Flora of Andhra Pradesh. Vol. 2. ; Matthew, K.M., The Flora of Tamil Nadu Carnatic, Vol.3 (2). Diocesan Press, Madras. 1983.

Morphology

Commonly known as “Sand Potato Bush” is a bushy shrub, 1-1.5 m tall, or a small tree up to 4 m tall, entirely hairless. Main branches are rough with stipule-scars and reduced scaly leaves; leaf-bearing branchlets fascicled, 4-7 mm long, few-leaved, often deciduous. Leaves are elliptic, ovate-elliptic, curved oblong-elliptic to round or obovate, obliquely wedge-shaped, pointed, blunt to rounded at base, pointed, rounded or blunt and apiculate at tip, 5-23 x 4-17 mm, membranous, hairless, pale glaucous beneath; leaf-stalks 1-3 mm long. Flowers are borne directly on older branches, unisexual, in many-flowered glomerules, often stalked. Male flowers occur at proximal axils; flower-stalks 3-9 mm long, thread-like; sepals 3 + 3, obovate, ovate or round, 0.6-1.2 x 0.4-1 mm; disc annular, about 0.5 mm across, 6-lobed; stamens 6, protruding; filaments 1.5-2.8 mm long, free, thread-like. Female flowers occur at distal axils; flower-stalks 8-37 mm long, thread-like; sepals 6, broadly ovate to elliptic, 2-2.2 x 1.6-1.8 mm, scarious along margins; disc subentire to 6-lobed, about 2 mm across, flat. Fruits are nearly spherical, 6-8 x 10-11 mm, 3-lobed, crustaceous, wrinkled, with longitudinal nervation. Sand Potato Bush is found in Semideciduous and scrub forests, up to 1000 m, common, in Telangana, Andhra Pradesh and Tamil Nadu, Sri Lanka and East Africa. Flowering: February-October.

Flowering: February, April to July, and September (Fig; A-B).

Synthesis of Silver Nanoparticles from Leaves of *Phyllanthus pinnatus*

This study explores an environmentally friendly method for synthesizing silver nanoparticles (AgNPs) using *Phyllanthus pinnatus* leaf extract. Silver nitrate ($AgNO_3$) was reduced by bioactive compounds extracted from *P. pinnatus* leaves using methanol. The green synthesis process was carried out over 48 hours at a controlled temperature of 68°C with continuous agitation. A visible color change from yellow to brown indicated the successful formation of silver nanoparticles. This color shift is attributed to the excitation of surface plasmon resonance (SPR), and a characteristic absorption peak at 445 nm (Fig.) confirmed the presence of AgNPs. The production of AgNPs via this green chemistry approach ensures a sustainable and non-toxic synthesis pathway.

An alternative method was also employed where the synthesis was conducted at a slightly lower temperature of 68 °C for 48 hours, with continuous agitation. This slower reaction approach also resulted in successful nanoparticle formation, as evidenced by similar optical properties and color change, suggesting that both thermally accelerated and time-prolonged synthesis pathways are viable for AgNP preparation using *P. pinnatus*. The synthesized nanoparticles were labeled and stored at 4 °C for further analysis.

The overall process demonstrated an eco-friendly, sustainable, and non-toxic approach, relying solely on the phytochemicals present in *P. pinnatus* for the reduction and stabilization of silver ions into stable nanoparticles. This confirms the plant’s potential as a green reducing and capping agent, aligning with environmentally conscious nanotechnology practices.

Characterization of Silver Nano Particles from *P. pinnatus*

UV–Visible Absorption Spectroscopy

The formation and stability of *P. pinnatus*-derived silver nanoparticles (PP-AgNPs) were confirmed by UV–Vis spectral analysis (Figure 3).

A prominent absorption peak was observed at 445 nm, which corresponds to the characteristic surface plasmon resonance (SPR) of AgNPs. This confirms the reduction of silver ions (Ag^{+}) to elemental silver (Ag^{0}) by phytochemicals present in the leaf extract (Figure 3). The absorption in the 400–460 nm range is typical for spherical nanoparticles, supporting the successful synthesis of AgNPs through the green route.

Fourier Transform Infrared Spectroscopy (FTIR)

FTIR analysis (Figure: FTIR Spectrum) was performed to identify the functional groups responsible for the reduction and capping of AgNPs. The spectrum displayed a broad peak at 3238.88 cm^{-1}, indicating O–H stretching of hydroxyl groups from phenolic compounds or alcohols. Peaks at 2917.77 cm^{-1} correspond to C–H stretching vibrations (Figure 4).

A strong peak at 1598.60 cm^{-1} is attributed to the N–H bending of primary amines or aromatic ring vibrations. Other prominent peaks at 1401.03 cm^{-1}, 1278.67 cm^{-1}, and 1181.90 cm^{-1} may represent C–N stretching of amines, confirming the role of proteins or alkaloids in stabilizing AgNPs (Figure 5-13). Peaks in the range of 1000–1100 cm^{-1} further indicate the presence of C–O–C or C–O–H functional groups. Collectively, these data confirm that phenols, flavonoids, and proteins from the leaf extract acted as both reducing and capping agents during AgNP formation.

X-ray Diffraction (XRD) Analysis

XRD analysis (Figure: XRD Graph – CSIR-IICT Hyderabad) confirmed the crystalline nature of the synthesized AgNPs. The diffraction peaks observed at 2θ values of 27.28°, 29.68°, 32.26°, 38.24°, 43.16°, 46.18°, and 50.07° were indexed to the (110), (111), (200), and (220) planes of face-centered cubic (fcc) silver crystals, as per JCPDS data.

The most intense peak at 38.24° corresponds to the (111) plane, which is characteristic of metallic silver nanoparticles. Using the Debye-Scherrer equation, the average crystalline size of the nanoparticles was calculated to be approximately 15–20 nm, which closely aligns with the size observed in TEM imaging (Figure 5).

Scanning Electron Microscopy (SEM)

SEM micrographs (Figure: SEM Image) revealed the surface morphology of PP-AgNPs. The images showed aggregated and irregularly shaped nanoparticle clusters with rough surfaces.

The particles appeared to be layered and densely packed, suggesting partial agglomeration. However, the surface morphology supports successful nanoparticle formation. The SEM imaging was conducted at a magnification of ×700, confirming the nanoscale nature of the synthesized particles (Figure 6).

Transmission Electron Microscopy (TEM)

TEM analysis (Figure: TEM Images) was performed to study the detailed size and shape of individual AgNPs. The particles were found to be spherical, well-dispersed, and had an average size ranging between 10.76 nm and 15.32 nm, confirming their nanoscale dimension. Most particles were uniformly distributed with minimal aggregation, indicating effective stabilization by biomolecules from the *P. pinnatus* extract. The size range observed in TEM images is consistent with the results obtained from XRD analysis (Figure 7).

Zeta Potential and Surface Stability

Zeta potential measurements (Figure: Zeta Potential Graph and Results Table) revealed that the synthesized PP-AgNPs exhibited a mean zeta potential value of −2.0 mV.

Although a higher absolute value (±30 mV) generally indicates strong electrostatic stability, the slightly negative charge here suggests moderate stability of the nanoparticle suspension, potentially stabilized via steric hindrance by capping biomolecules rather than pure electrostatic repulsion (Figure 8 & Figure 9). The electrophoretic mobility value was recorded as −0.000015 cm^2/Vs, further supporting colloidal stability in the aqueous medium.

DPPH Free Radical Scavenging Activity

The free radical scavenging activity of *Phyllanthus pinnatus*-mediated silver nanoparticles was evaluated using the 1,1-diphenyl-2-picrylhydrazyl (DPPH) radical scavenging assay, following the method described by Ebrahimzadeh and Bahramian (2009). This method is based on the reduction of the DPPH radical in methanol solution by hydrogen-donating antioxidants, resulting in the conversion of the deep purple-colored DPPH solution to a yellow-colored non-radical form (DPPH-H). This color change indicates the antioxidant activity of the test sample and is measured spectrophotometrically at 517 nm. In the present study, freshly prepared 0.2 mM DPPH solution in methanol was used, and the optical density was adjusted to 0.8 at 517 nm to ensure consistency.

Varying concentrations of *Phyllanthus pinnatus* silver nanoparticles (10, 25, 50, 75, and 100 µg/ml) were tested, and ascorbic acid (Vitamin C) was used as a standard reference antioxidant. After incubation of the sample-DPPH mixture for 30 minutes, the absorbance was recorded, and the percentage inhibition was calculated using the standard formula. The results showed that ascorbic acid exhibited high antioxidant activity, with the percentage of DPPH radical inhibition increasing from 19.21% at 10 µg/ml to 84.94% at 100 µg/ml. In comparison, *Phyllanthus pinnatus* silver nanoparticles displayed moderate but concentration-dependent antioxidant activity, with inhibition increasing from 8.83% at 10 µg/ml to 72.18% at 100 µg/ml.

These findings indicate that while the antioxidant potential of *Phyllanthus pinnatus* silver nanoparticles is lower than that of ascorbic acid, the nanoparticles still possess significant radical scavenging ability, suggesting their potential application as natural antioxidant agents.

Hydrogen peroxide radical scavenging (H_2O_2) Assay

The hydrogen peroxide radical scavenging activity of *Phyllanthus pinnatus*-mediated silver nanoparticles was evaluated using the method described by Ruch *et al.,* (1984). In this assay, a 40 mM hydrogen peroxide solution was prepared in 1M phosphate buffer at pH 7.4, and the concentration of hydrogen peroxide was confirmed by measuring its absorbance at 230 nm using a spectrophotometer. Different concentrations of *Phyllanthus pinnatus* silver nanoparticles, ranging from 10 to 100 µg/ml, were prepared in distilled water and added to the hydrogen peroxide solution. After 10 minutes of incubation, the absorbance of the reaction mixture was recorded at 230 nm, using phosphate buffer without hydrogen peroxide as a blank. The percentage of hydrogen peroxide scavenging activity was calculated using the formula:

% scavenging activity = [(A control – A sample) / A control] × 100,

Where A control represents the absorbance of the hydrogen peroxide solution without any sample, and A sample represents the absorbance of the test sample. All experiments were performed in triplicate for accuracy.

The results showed that ascorbic acid, used as a standard antioxidant, exhibited strong hydrogen peroxide scavenging activity, increasing from 19.23% at 10 µg/ml to 86.41% at 100 µg/ml, indicating a clear concentration-dependent response. In comparison, the *Phyllanthus pinnatus* silver nanoparticles demonstrated moderate yet significant scavenging activity. The percentage inhibition increased from 10.26% at 10 µg/ml to 73.21% at 100 µg/ml, also following a concentration-dependent trend. Although the antioxidant activity of *Phyllanthus pinnatus* silver nanoparticles was lower than that of ascorbic acid, the nanoparticles still showed notable ability to scavenge hydrogen peroxide radicals.

These findings suggest that *Phyllanthus pinnatus*-mediated silver nanoparticles possess effective antioxidant properties and could potentially serve as natural radical scavengers, contributing to oxidative stress reduction.

Anti-Microbial Activity

Antibacterial activity

The antibacterial efficacy of silver nanoparticles (AgNPs) synthesized using *Phyllanthus pinnatus* methanolic leaf extract was evaluated against four pathogenic bacterial strains—two Gram-positive (*Staphylococcus aureus* ATCC 25923 and *Streptococcus pneumoniae* ATCC 33400) and two Gram-negative (*Escherichia coli* ATCC 25922 and *Pseudomonas aeruginosa* ATCC 27853)—using the agar well diffusion method. The study was designed to assess the concentration-dependent antibacterial potential of PP-

AgNPs at four test concentrations (25, 50, 75, and 100 µg), and the results were directly compared with those of the standard antibiotic Ampicillin at the same concentrations.

The green-synthesized AgNPs demonstrated significant antibacterial activity against all tested strains, with the zone of inhibition (ZOI) increasing proportionally with concentration. Against *Staphylococcus aureus*, the inhibition zones produced by AgNPs were 18 mm, 20 mm, 22 mm, and 24 mm for the four concentrations, respectively. These values were consistently higher than those of Ampicillin, which exhibited ZOIs of 17 mm to 22 mm across the same concentrations (Figure 14 & Table 5). The antimicrobial action of AgNPs against *Escherichia coli* was even more pronounced, with inhibition zones ranging from 21 mm to 26 mm, as compared to Ampicillin's range of 16 mm to 21 mm. The results suggest that the nanoparticles possess superior activity against this Gram-negative pathogen, which is often resistant to standard antibiotics.

Interestingly, *Streptococcus pneumoniae*, a Gram-positive organism known for its resilience, responded remarkably well to the nanoparticle treatment. The ZOIs observed for PP-AgNPs were 22 mm, 23 mm, 25 mm, and 27 mm from lowest to highest concentration, in contrast to Ampicillin, which only produced inhibition zones of 11 mm to 17 mm. This result clearly indicates the enhanced potential of AgNPs as a powerful antimicrobial agent against this respiratory pathogen. Among all tested organisms, *Pseudomonas aeruginosa*, a notoriously drug-resistant Gram-negative bacterium, also showed a strong inhibitory response to PP-AgNPs. The measured zones of inhibition ranged from 22 mm at 25 µg to 28 mm at 100 µg, whereas Ampicillin showed significantly lower effectiveness with inhibition zones of 12 mm to 18 mm (Figure15 & Table *5*) Table 6: Anti-Bacterial Activity of silver nanoparticle synthesized from PP extract. Zone of Inhibition represented in mm..

These findings highlight the broad-spectrum antibacterial properties of the green-synthesized silver nanoparticles. The higher efficacy of PP-AgNPs in comparison to Ampicillin across all bacterial strains and concentrations may be attributed to the small particle size (10–15 nm), increased surface area, and the bioactive phytochemicals from *P. pinnatus* that likely serve as capping and stabilizing agents, enhancing the nanoparticles' interaction with bacterial membranes. The synergistic effect of silver ions and plant-derived biomolecules possibly disrupts cell wall integrity, inhibits DNA replication, and induces oxidative stress in microbial cells, thereby leading to effective bacterial inhibition.

In conclusion, the AgNPs synthesized using *Phyllanthus pinnatus* leaf extract demonstrate promising and consistent antibacterial activity across multiple bacterial species. The results not only validate the traditional use of the plant for antimicrobial purposes but also suggest that these green-synthesized nanoparticles could serve as a potent, sustainable, and eco-friendly alternative to conventional antibiotics, especially in the era of increasing antibiotic resistance.

Minimum Inhibitory Concentration (MIC)

The Minimum Inhibitory Concentration (MIC) is a critical parameter in antimicrobial evaluation, defining the lowest concentration of a compound required to inhibit visible microbial growth after overnight incubation. In the present study, MIC values were determined for silver nanoparticles (AgNPs) synthesized using *Phyllanthus pinnatus* methanolic leaf extract, and the results were compared with those of the standard antibiotic Ampicillin. MIC tests were conducted against four bacterial strains *Staphylococcus aureus*, *Escherichia coli*, *Streptococcus pneumoniae*, and *Pseudomonas aeruginosa* by measuring optical density (OD) at 600 nm following incubation with serial concentrations (5, 10, 25, 50, 100, and 200 µg/mL) of the test compounds. For *Staphylococcus aureus*, a Gram-positive organism frequently associated with skin and wound infections, the PP-AgNPs demonstrated a clear dose-dependent inhibition of growth. The OD values decreased steadily from 0.463 at 5 µg/mL to 0.264 at 200 µg/mL, indicating increasing bacterial suppression with increasing nanoparticle concentration. In comparison, Ampicillin showed more pronounced antibacterial activity against *S. aureus*, with OD values dropping from 0.346 at 5 µg/mL to 0.097 at 200 µg/mL.

While the standard antibiotic proved slightly more effective at higher concentrations, the AgNPs still showed significant inhibitory potential, suggesting their usefulness especially in resistance-prone cases where traditional antibiotics may be less effective.

Against *Escherichia coli*, a Gram-negative enteric pathogen, PP-AgNPs also displayed strong antimicrobial activity. The OD values decreased from 0.413 at 5 µg/mL to 0.213 at 200 µg/mL, highlighting the

concentration-dependent inhibition pattern. In parallel, Ampicillin showed OD values from 0.327 to 0.098 over the same concentration range, again confirming its strong activity, but closely paralleled by the green-synthesized nanoparticles. The comparable performance of AgNPs against *E. coli*, despite the bacteria's outer membrane barrier, suggests the effective permeability and interaction of the nanoparticles with bacterial surfaces.

Interestingly, in the case of *Streptococcus pneumoniae*, the AgNPs demonstrated particularly impressive inhibitory effects. The OD readings declined from 0.421 at 5 µg/mL to 0.212 at 200 µg/mL, showcasing efficient bacteriostatic activity across all tested concentrations. This is noteworthy as *S. pneumoniae* is a known respiratory pathogen that has developed resistance to several conventional antibiotics. The nanoparticle efficacy observed here suggests their potential application in targeting such drug-resistant strains.

Similarly, for *Pseudomonas aeruginosa*, an opportunistic Gram-negative pathogen notorious for its multidrug resistance and persistence in clinical settings, the AgNPs showed significant antimicrobial action. The OD values dropped from 0.445 to 0.231, demonstrating their ability to effectively inhibit this resilient organism. This result is particularly promising, as *P. aeruginosa* typically exhibits low sensitivity to antibiotics like Ampicillin, and the performance of AgNPs suggests their potential to fill gaps left by traditional treatments.

Overall, while Ampicillin exhibited slightly superior inhibitory activity against *S. aureus* and *E. coli*, the silver nanoparticles synthesized using *Phyllanthus pinnatus* leaf extract performed remarkably well across all four tested strains. The MIC results reinforce the outcomes observed in agar well diffusion assays and confirm the broad-spectrum efficacy of PP-AgNPs. Their performance against both Gram-positive and Gram-negative bacteria, particularly drug-resistant strains like *P. aeruginosa* and *S. pneumoniae*, highlights the potential of these biosynthesized nanoparticles as a sustainable and effective antimicrobial alternative. Additionally, the use of green synthesis eliminates the need for toxic chemical reducing agents, enhancing the biocompatibility and environmental safety of the resulting nanomaterials.

These findings collectively suggest that *Phyllanthus pinnatus*-mediated silver nanoparticles are not only effective but also versatile in targeting a wide range of bacterial pathogens, making them suitable candidates for further development in antimicrobial therapies, particularly in the era of escalating antibiotic resistance.

Anti-Fungal Activity

The antifungal potential of the test compound prepared from *Phyllanthus pinnatus* leaf extract was assessed against two pathogenic fungal strains: *Candida albicans* (MTCC 183) and *Aspergillus niger* (MTCC, IMTECH, Chandigarh). The experiment was carried out using the agar well diffusion method on Sabouraud Dextrose Agar (SDA) plates, which were inoculated using the spread plate technique. Following a 48-hour incubation period at 37 ± 2°C, the plates were examined for zones of inhibition surrounding the wells, which reflect the antifungal efficacy of the test samples.

The standard antifungal agent Fluconazole was used as a positive control to establish baseline inhibitory activity. Fluconazole exhibited strong antifungal activity against both fungal strains across all tested concentrations. Against *Candida albicans*, it produced zones of inhibition measuring 10 mm, 12 mm, 14 mm, and 17 mm at 25, 50, 75, and 100 µg, respectively. *Aspergillus niger* demonstrated a slightly higher sensitivity, with corresponding inhibition zones of 13 mm, 14 mm, 16 mm, and 19 mm, indicating that Fluconazole was consistently effective even at lower concentrations.

In contrast, the test compound derived from *P. pinnatus* demonstrated a more selective and concentration-dependent antifungal effect. For *Candida albicans*, no zone of inhibition was observed at lower concentrations (25 and 50 µg), indicating limited activity at these levels.

However, moderate antifungal activity emerged at higher concentrations, with inhibition zones of 11 mm at 75 µg and 12 mm at 100 µg, suggesting that effective antifungal activity begins to manifest only beyond a threshold concentration.

The response against *Aspergillus niger* was even more limited. No inhibition was observed at 25, 50, or 75 µg concentrations, and only a single zone of 12 mm was recorded at the highest tested concentration of 100 µg, indicating marginal susceptibility. This suggests that the active constituents within the PP-derived compound have weaker antifungal properties against filamentous fungi like *A. niger* compared to yeast-like fungi such as *C. albicans*.

Schematic representation for plant-mediated green synthesis of nanoparticles

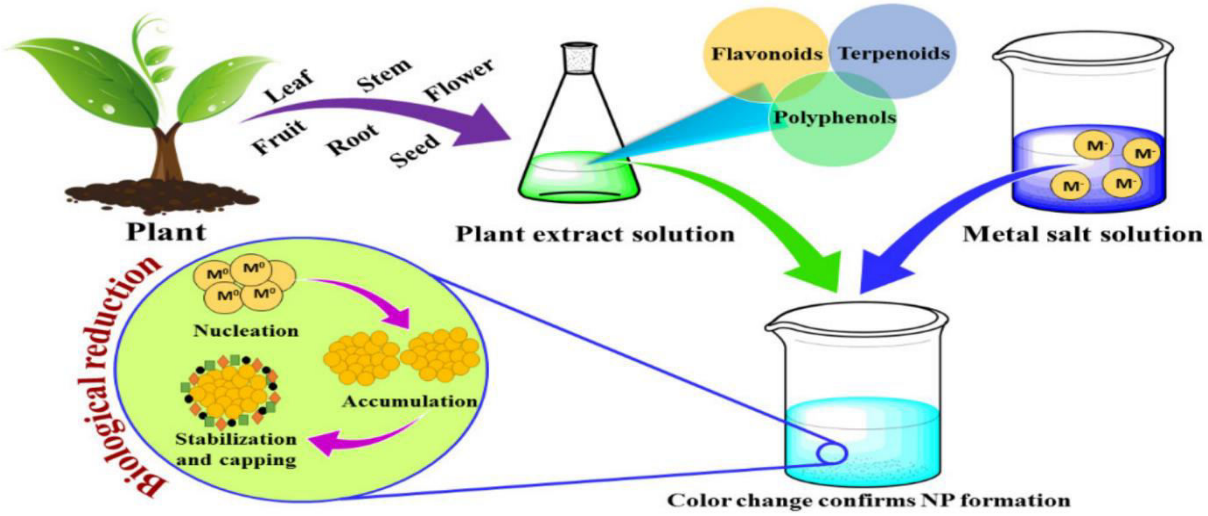

Fig.1 Habitat of *P. pinnatus*

Fig.2 Synthesis of silver nano particles from *P. pinnatus*

Fig.3 UV–Visible absorption spectrum of silver nanoparticles synthesized using *P. pinnatus* extract. A characteristic SPR peak at 445 nm confirms the formation of AgNPs. The peak list table alongside the graph shows absorbance values at various wavelengths.

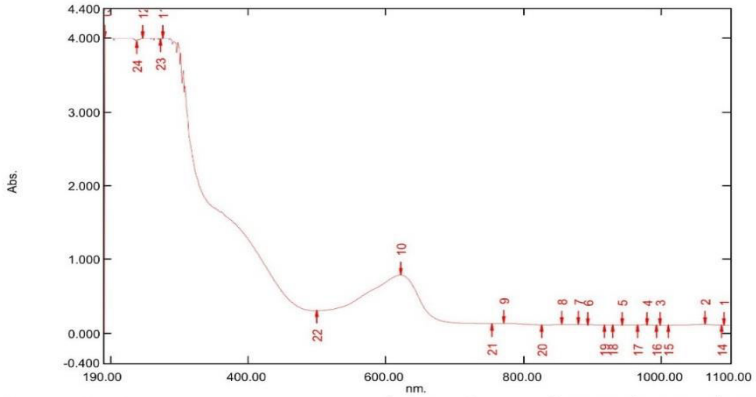

Measurement Properties	
Wavelength Range (nm.):	190.00 to 1100.00
Scan Speed:	Medium
Sampling Interval:	1.0
Auto Sampling Interval:	Enabled
Scan Mode:	Auto
Instrument Properties	
Instrument Type:	UV-1800 Series
Measuring Mode:	Absorbance
Slit Width:	1.0 nm
Light Source Change Wavelength:	340.8 nm
S/R Exchange:	Normal
Attachment Properties	
Attachment:	None
Sample Preparation Properties	
Weight:	
Volume:	
Dilution:	
Path Length:	
Additional Information:	

No.	P/V	Wavelength	Abs.	Description
1	▲	1092.00	0.110	
2	▲	1064.00	0.122	
3	▲	999.00	0.111	
4	▲	980.00	0.117	
5	▲	944.00	0.115	
6	▲	894.00	0.118	
7	▲	879.00	0.120	
8	▲	855.00	0.119	
9	▲	772.00	0.133	
10	▲	622.00	0.790	
11	▲	276.00	4.000	
12	▲	246.00	4.000	
13	▲	192.00	4.000	
14	▼	1088.00	0.109	
15	▼	1011.00	0.110	
16	▼	994.00	0.109	
17	▼	966.00	0.112	
18	▼	929.00	0.113	
19	▼	918.00	0.113	
20	▼	827.00	0.114	
21	▼	755.00	0.131	
22	▼	499.00	0.305	
23	▼	273.00	3.982	
24	▼	238.00	3.962	

Figure.4 Fourier Transform Infrared (FTIR) spectrum of green-synthesized silver nanoparticles (AgNPs) using *Phyllanthus pinnatus* leaf extract. The peaks at 3238.88 cm^{-1}, 2917.77 cm^{-1}, 1598.60 cm^{-1}, and 1401.03 cm^{-1} indicate the presence of hydroxyl, amine, and phenolic groups, suggesting the role of plant biomolecules in nanoparticle reduction and stabilization.

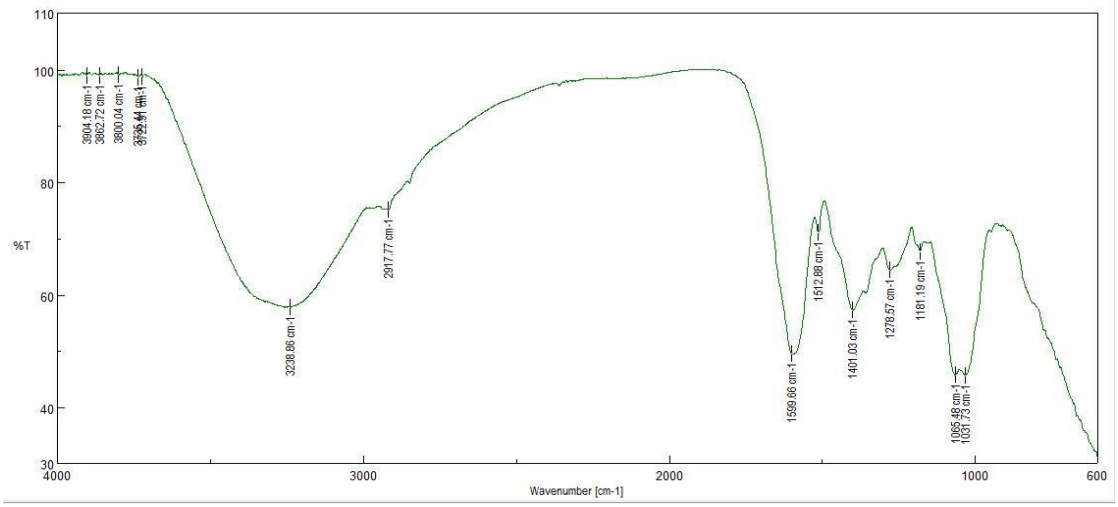

Figure.0 X-Ray Diffraction (XRD) spectrum of synthesized silver nanoparticles. The diffraction peaks at 2θ values of 27.28°, 29.68°, 32.26°, 38.24°, and 43.16° correspond to the (111), (200), and (220) planes of face-centered cubic (fcc) silver, confirming crystalline structure.

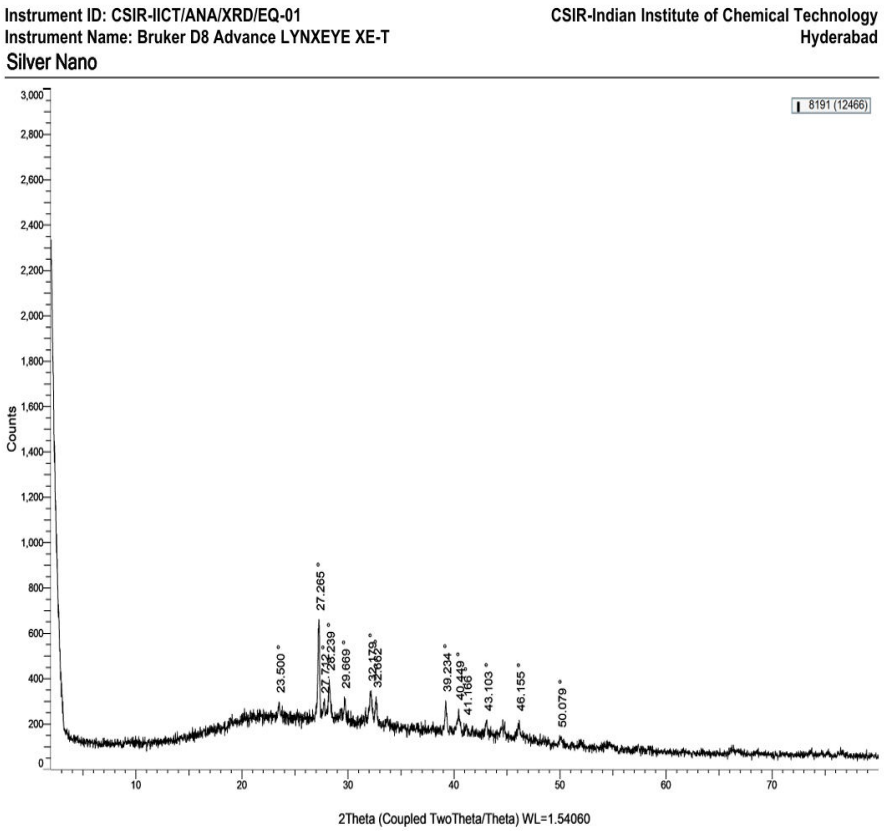

Figure.6 Scanning Electron Microscopy (SEM) image of *P. pinnatus*-derived silver nanoparticles. The particles show irregular morphology with some agglomeration, indicating surface texture and nanostructure aggregation at ×700 magnification and 50 µm scale.

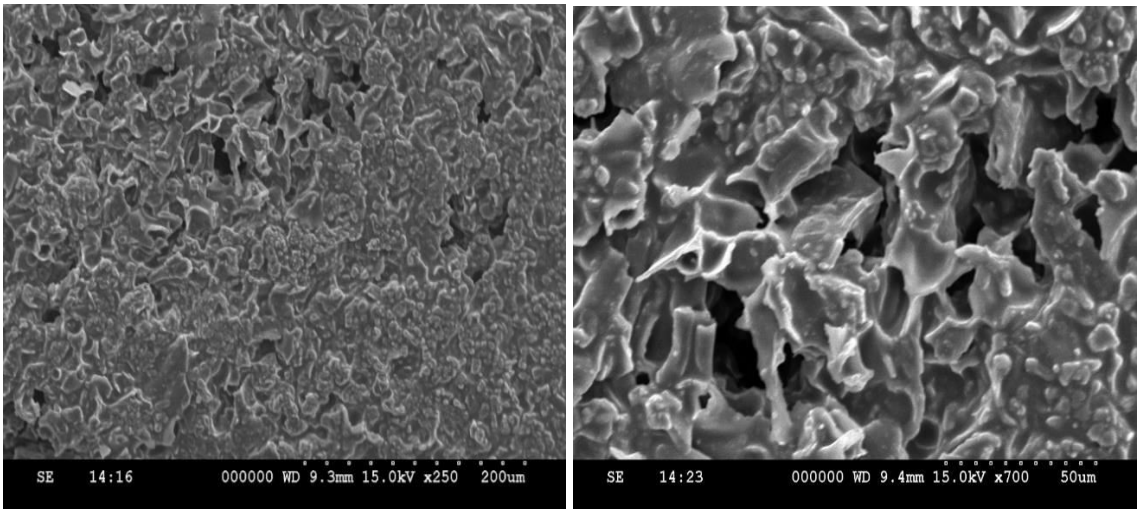

Figure.7 Transmission Electron Microscopy (TEM) images of biosynthesized silver nanoparticles at different magnifications. The particles appear spherical, polydispersed, and well-dispersed with an average size of approximately 10–15 nm, validating nanoscale.

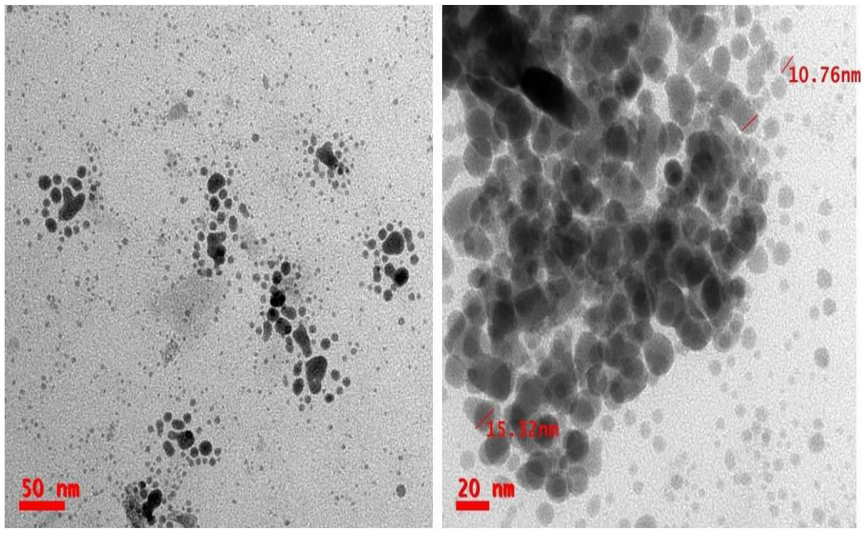

Figure.8 Graphical representation of zeta potential distribution of biosynthesized AgNPs. The narrow peak centered around −2.0 mV indicates relatively uniform surface charge and moderate suspension stability.

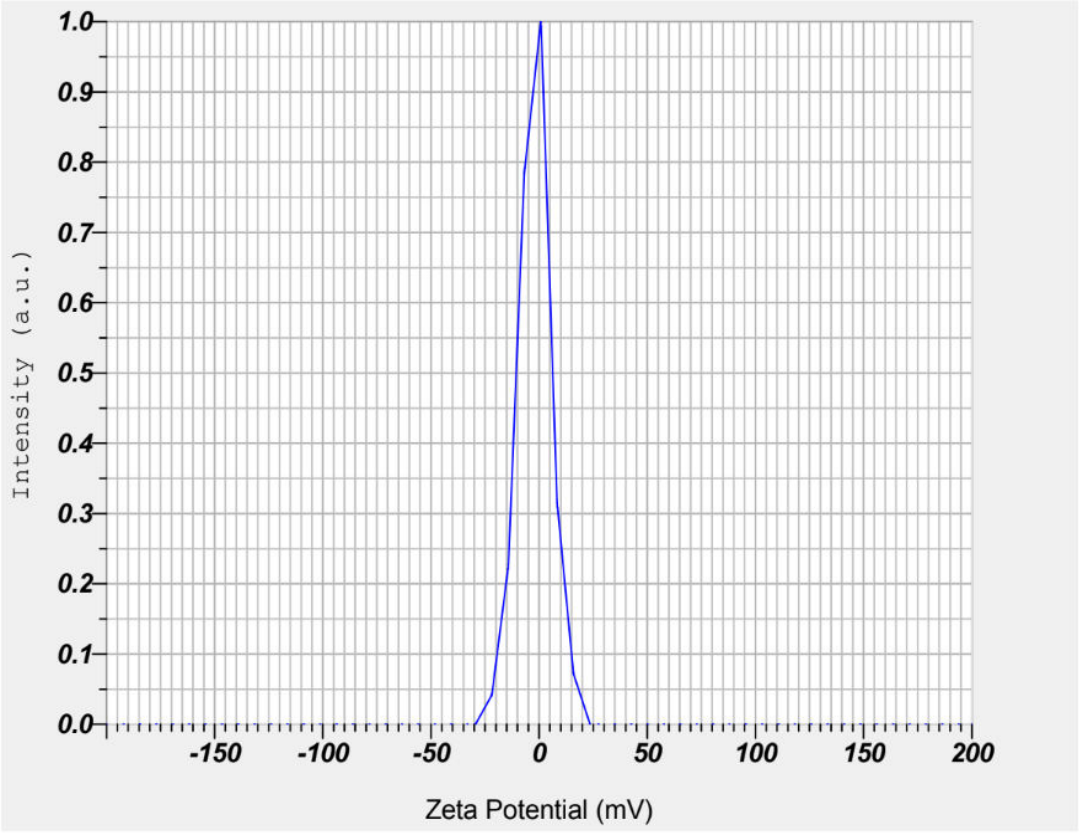

Figure.9 Zeta potential measurement results of green-synthesized AgNPs. The mean zeta potential value was recorded as −2.0 mV, indicating moderate colloidal stability, with electrophoretic mobility of −0.000015 cm²/Vs.

Measurement Results

202404101610000.nzt

Measurement Results

Date	:	10 April 2024 16:10:11
Measurement Type	:	Zeta Potential
Sample Name	:	BSANP-15BSA+20PX-ZETA
Temperature of the holder	:	25.0 deg. C
Viscosity of the dispersion medium	:	0.895 mPa.s
Conductivity	:	0.726 mS/cm
Electrode Voltage	:	3.3 V

Calculation Results

Peak No.	Zeta Potential	Electrophoretic Mobility
1	-2.0 mV	-0.000015 cm2/Vs
2	--- mV	--- cm2/Vs
3	--- mV	--- cm2/Vs

Zeta Potential (Mean)	:	-2.0 mV
Electrophoretic Mobility mean	:	-0.000015 cm²/Vs

Figure.10 DPPH Scavenging Activity of Ascorbic acid

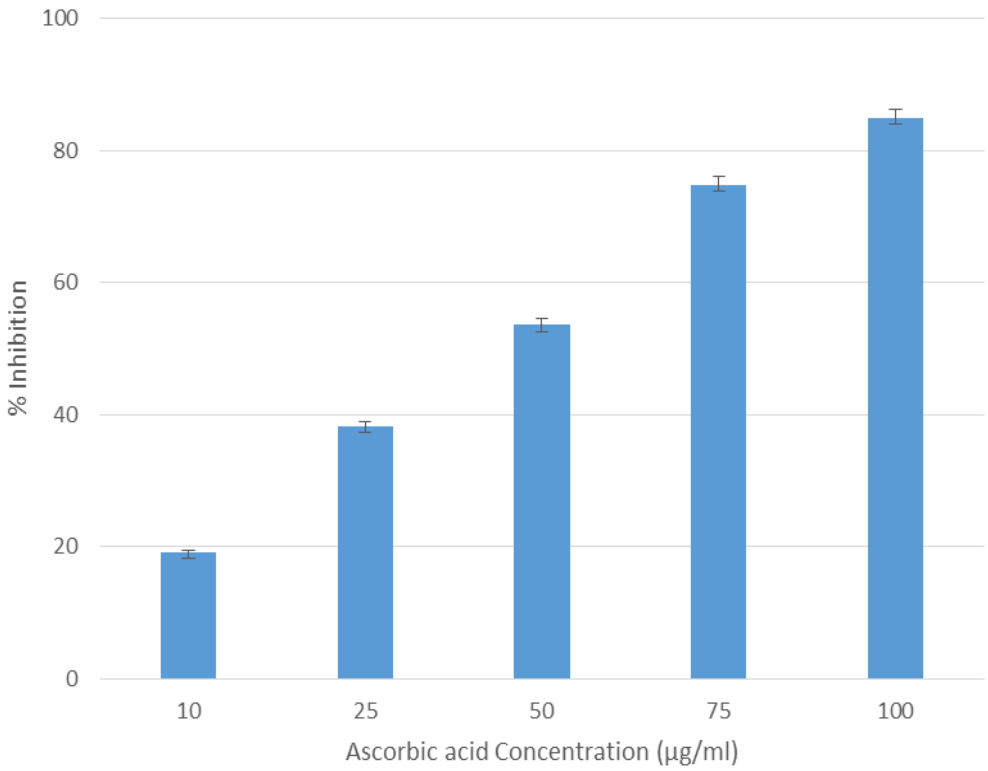

Figure.11 DPPH Scavenging Activity of PP-AgNPs

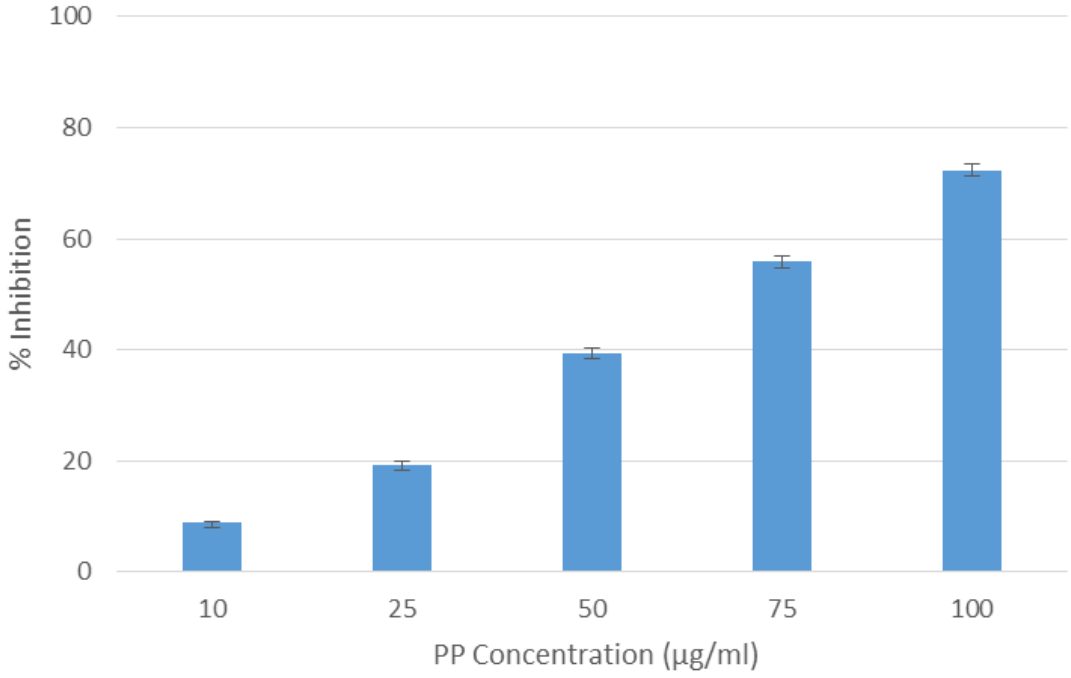

Figure.12 H_2O_2 Scavenging Activity of Ascorbic acid

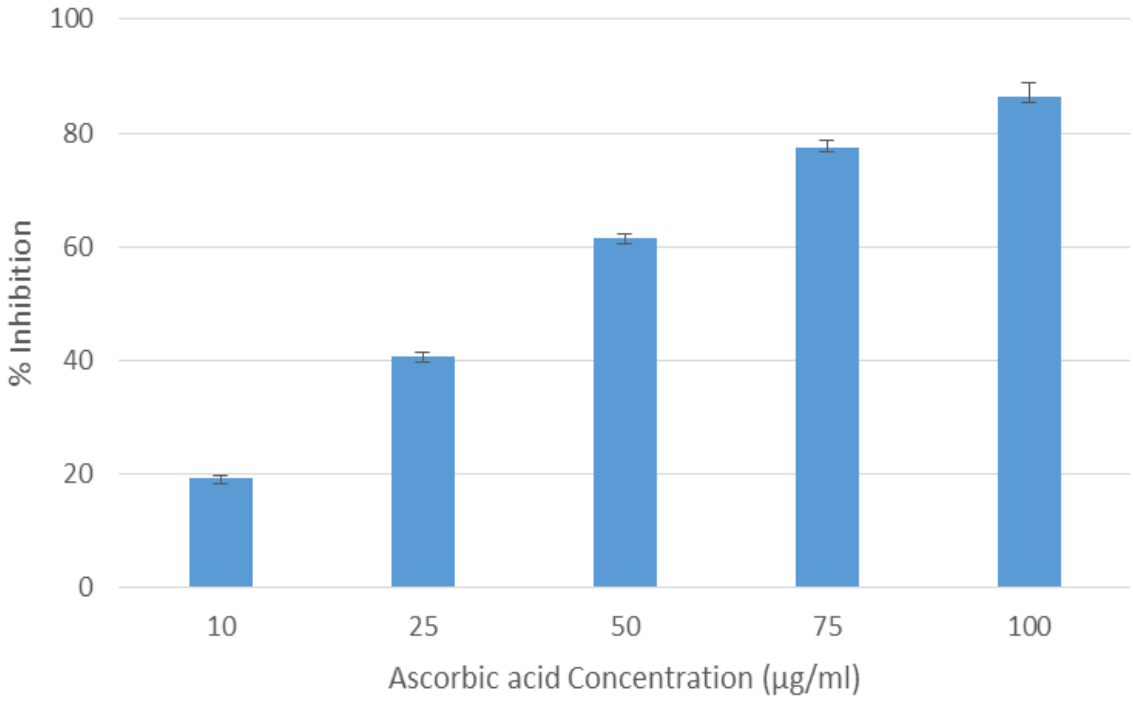

Figure.13 H_2O_2 Scavenging Activity of PP AgNPs

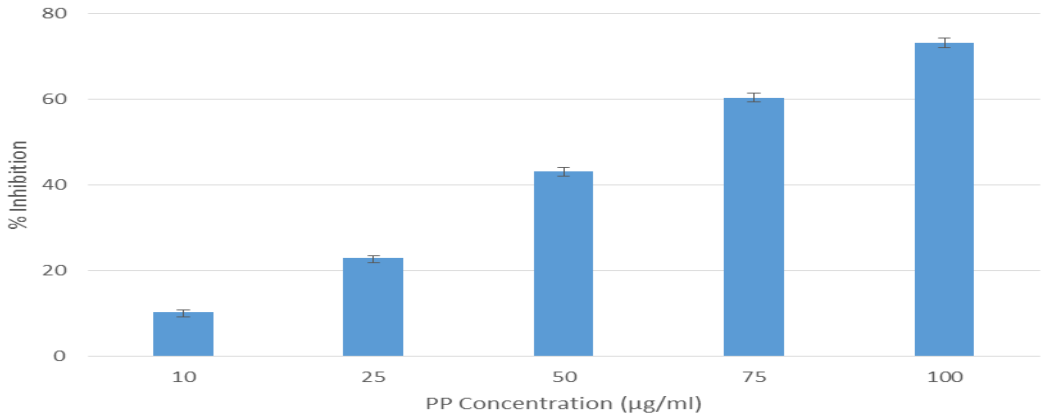

Figure.14 Anti-Bacterial Activity of Standard Ampicillin **(A)** *Staphylococcus aureus* **(B)** *E. coli* **(C)** *Streptococcus pneumonia* **(D)** *Pseudomonas aeruginosa*

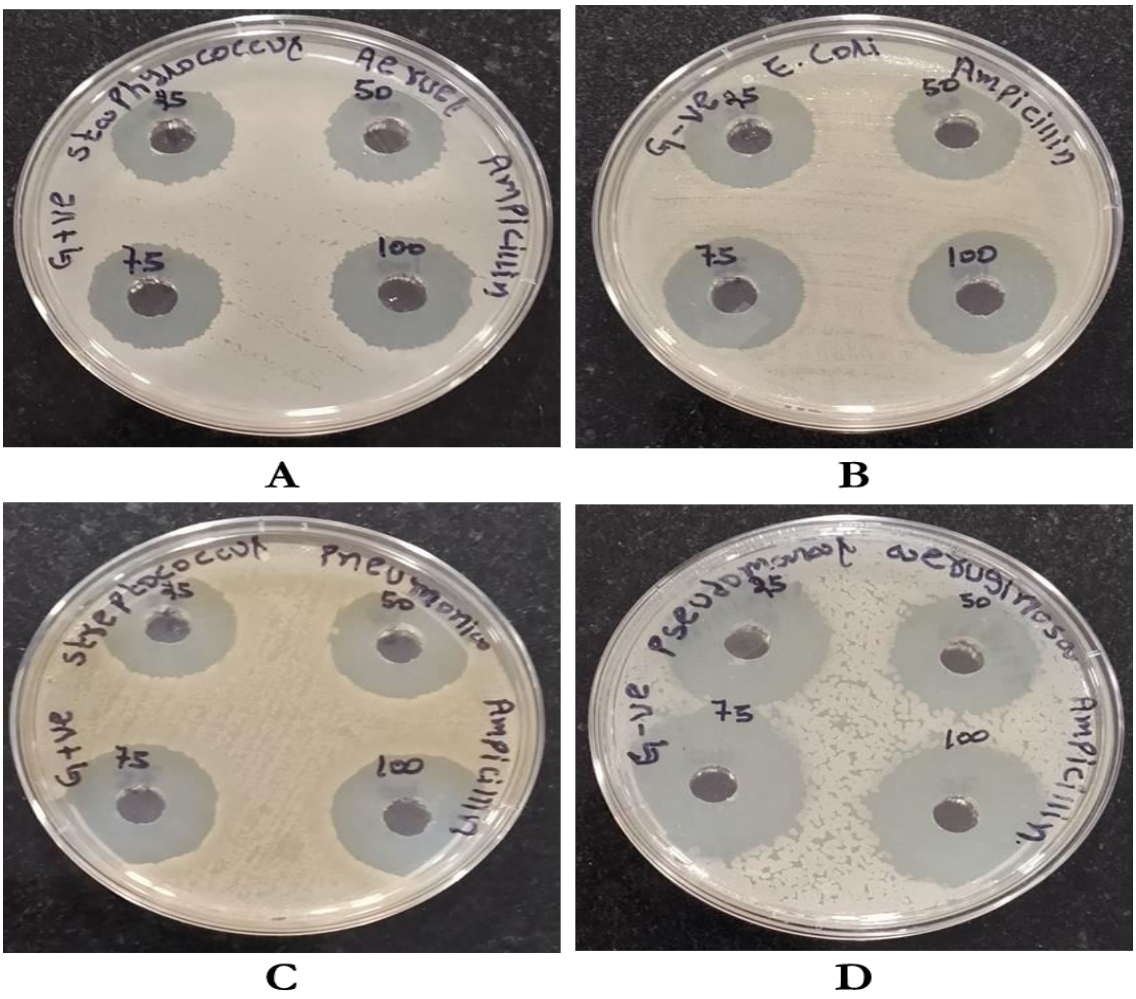

Figure.16 Anti-Bacterial Activity of PP (A) *Staphylococcus aureus* (B) *E. coli* (C) *Streptococcus pneumonia* (D) *Pseudomonas aeruginosa*

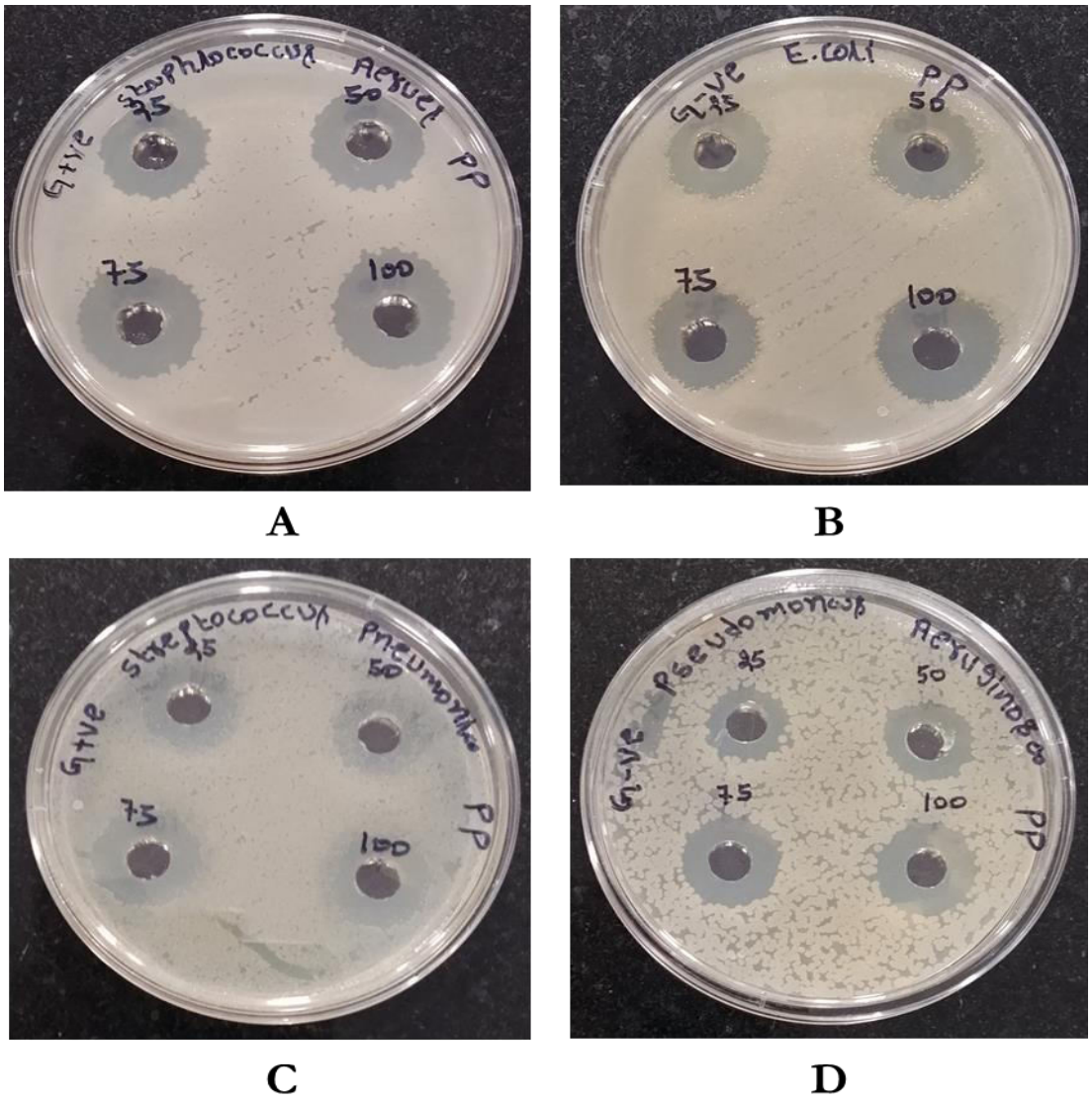

Figure.17 MIC activity of Ampicillin on *S. aureus*

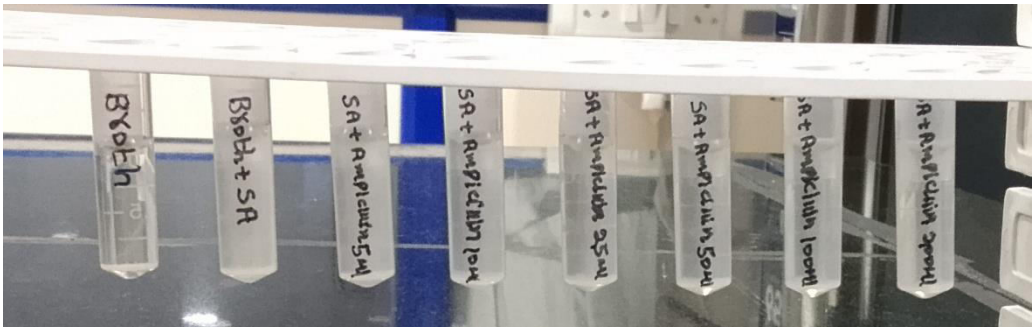

Figure.18 MIC activity of Ampicillin *on E. coli*

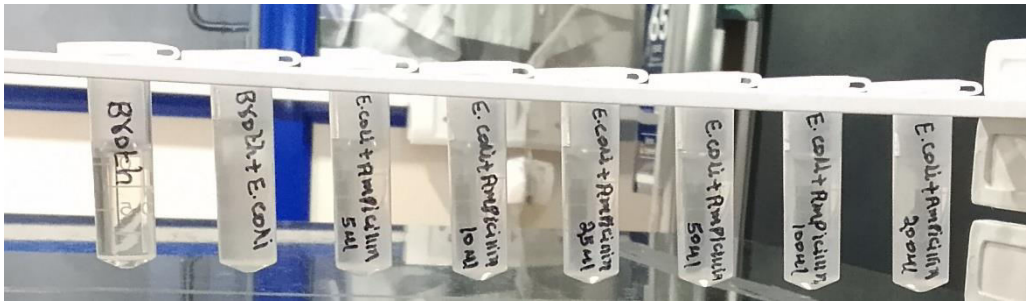

Figure.19 MIC activity of *PP* on *S. aureus*

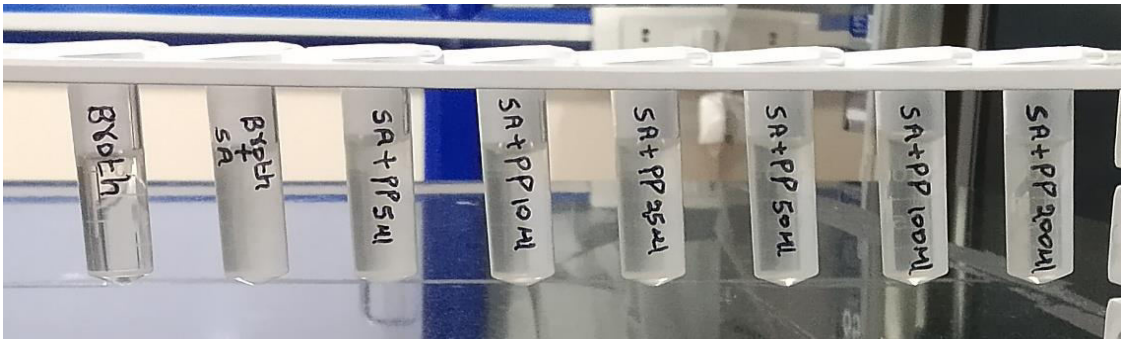

Figure.20 MIC activity of *PP* on *E. coli*

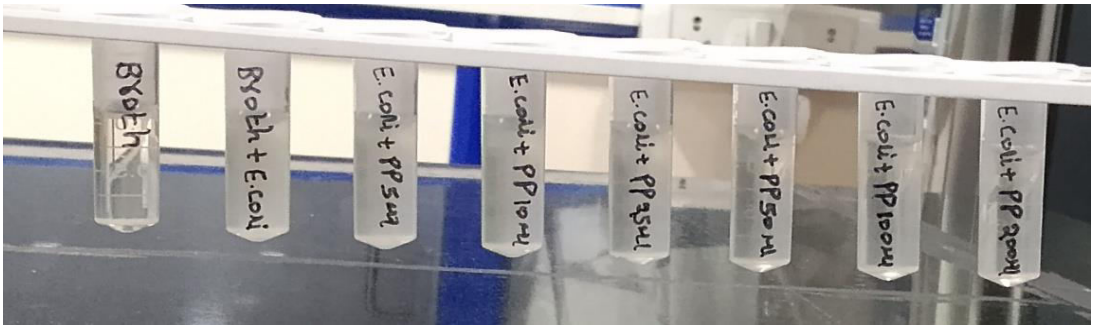

Figure.21 MIC activity of *PP* on *S. pneumoniae*

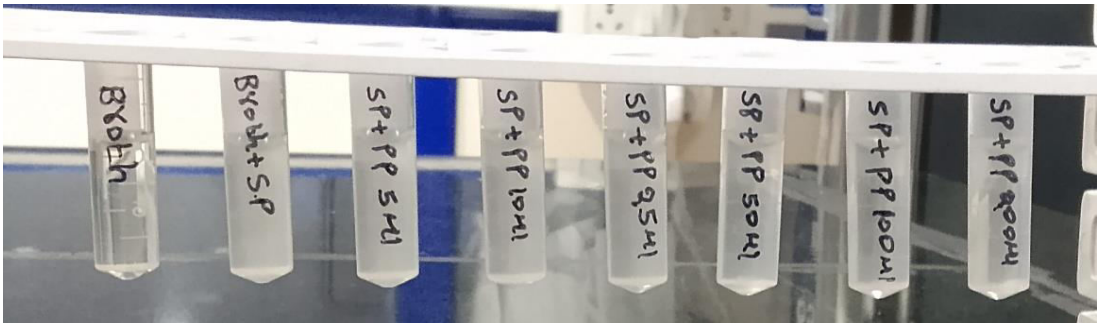

Figure.22 MIC activity of *PP* on *P.aeruginosa*

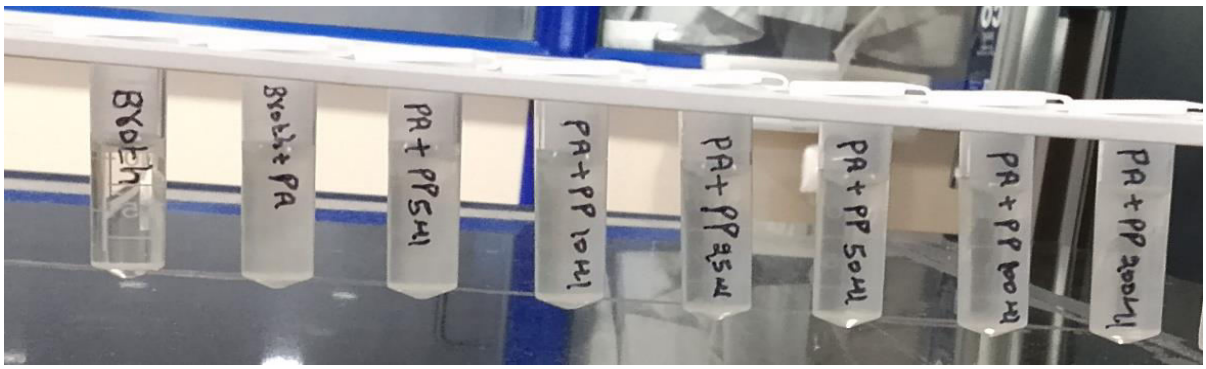

Figure.23 Anti-fungal Activity of Fluconozole A. *Candida albicans* B. *Aspergillus niger*

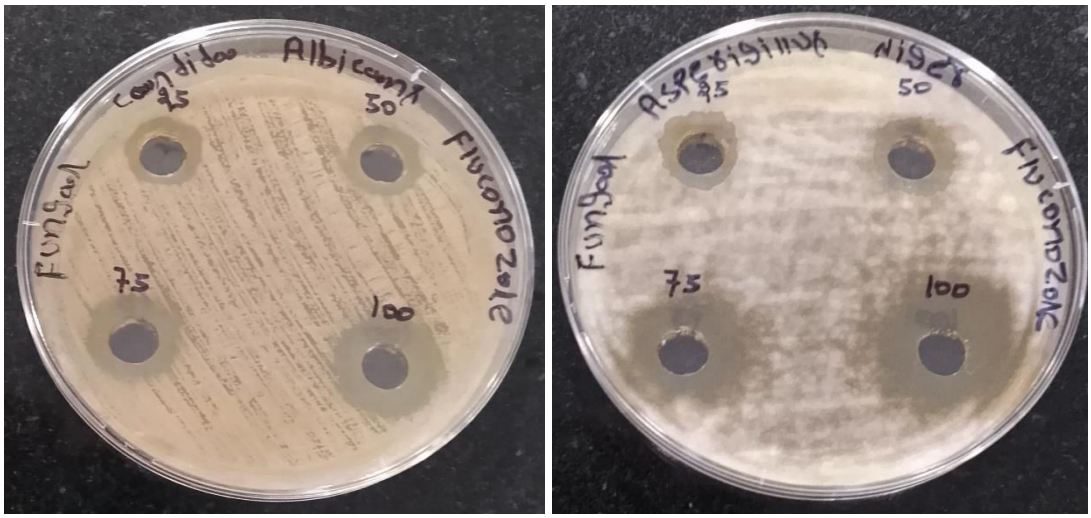

A **B**

Figure.24 Anti-fungal Activity of *PP*. A. *Candida albicans* B. *Aspergillus niger*

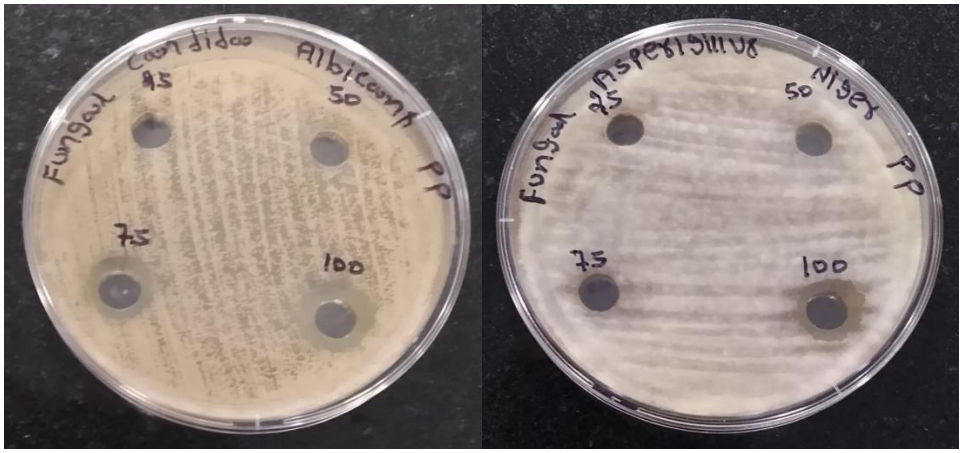

A **B**

Table.8 Classification of *P. pinnatus*

Kingdom	**Plantae**
Phylum	Streptophyta
Class	Equisetopsida
Subclass	Magnoliidae
Order	Malpighiales
Family	Phyllanthaceae
Genus	*Phyllanthus*
Species	*Phyllanthus pinnatus*

Table.1 DPPH Scavenging Activity of Ascorbic acid

Test Compound	Concentration (µg/ml)	% Inhibition
Ascorbic acid	10	19.21±0.185
	25	38.26±0.651
	50	53.58±0.964
	75	74.86±1.183
	100	84.94±1.376

Table.2 DPPH Scavenging Activity of PP-AgNPs

Test Compound	Concentration (µg/ml)	% Inhibition
PP-AgNPs	10	8.83±0.328
	25	19.26±0.657
	50	39.37±0.814
	75	55.84±1.085
	100	72.18±1.356

Table.3 H_2O_2 Scavenging Activity of Ascorbic acid

Test Compound	Concentration (µg/ml)	% Inhibition
Ascorbic acid	10	19.23±0.316
	25	40.68±0.638
	50	61.36±0.927
	75	77.54±1.162
	100	86.41±2.314

Table.4 H_2O_2 Scavenging Activity of PP AgNPs

Test Compound	Concentration (µg/ml)	% Inhibition
PPL-AgNPs	10	10.26±0.461
	25	22.89±0.668
	50	43.17±0.927
	75	60.35±1.094
	100	73.21±1.205

Table.0 Anti-Bacterial Activity of Standard Ampicillin. Zone of Inhibition represented in mm.

		Concentration (µg)/ Zone of Inhibition (mm)			
S No	**Strain**	**25**	**50**	**75**	**100**
1	*Staphylococcus aureus*	18	20	22	24
2	*E coli*	21	22	24	26
3	*Streptococcus pneumonia*	22	23	25	27
4	*Pseudomonas aeruginosa*	22	25	26	28

Table.6 Anti-Bacterial Activity of silver nanoparticle synthesized from PP extract. Zone of Inhibition represented in mm.

		Concentration (µg)/ Zone of Inhibition (mm)			
S No	**Strain**	**25**	**50**	**75**	**100**
1	*Staphylococcus aureus*	17	19	20	22
2	*E coli*	16	18	19	21
3	*Streptococcus pneumonia*	11	12	15	17
4	*Pseudomonas aeruginosa*	12	14	16	18

Table.7 MIC Activity of ampicillin against *S. Aureus* and *E. Coli*

Sr. No	**Type of bacteria**	**Concentration (µg/ml)**					
		5	**10**	**25**	**50**	**100**	**200**
1	**S aureus**	0.346	0.311	0.263	0.234	0.185	0.097
2	**E coli**	0.327	0.291	0.276	0.252	0.208	0.098

Table.8 MIC Activity of silver nanoparticle prepared from PP extract against *S. Aureus*, *E. Coli, S. pneumoniae, P. aeruginosa*

S. No	**Type of bacteria**	**Concentration (µg/ml)**					
		5	**10**	**25**	**50**	**100**	**200**
1	*S. aureus*	0.463	0.431	0.408	0.381	0.351	0.264
2	*E coli*	0.413	0.376	0.347	0.293	0.263	0.213
3	*S. pneumoniae*	0.421	0.404	0.378	0.346	0.257	0.212
4	*P. aeruginosa*	0.445	0.423	0.398	0.363	0.285	0.231

Table.9 Anti-fungal Activity of Fluconozole

		Concentration (µg)/ Zone of Inhibition (mm)			
S. No	**Strain**	**25**	**50**	**75**	**100**
1	*Candida albicans*	10	12	14	17
2	*Aspergillus niger*	13	14	16	19

Table.10 Anti-fungal Activity of *P. pinnatus* silver nano particle

		Concentration (µg)/ Zone of Inhibition (mm)			
S No	**Strain**	**25**	**50**	**75**	**100**
1	*Candida albicans*	0	0	11	12
2	*Aspergillus niger*	0	0	0	12

These findings collectively demonstrate that while the *P. pinnatus* test compound does exhibit some degree of antifungal activity, it is significantly less potent than Fluconazole, particularly at lower concentrations. The results also indicate that *C. albicans* is more susceptible to the test compound than *A. niger*, aligning with common patterns of differential fungal cell wall permeability and response to phytochemicals. Nevertheless, the moderate activity observed at higher doses suggests a potential for antifungal application, possibly in synergy with other agents or after further purification and enhancement of bioactive constituents.

Phyllanthus pinnatus belongs to a genus widely recognized for treating digestive, hepatic, renal, metabolic, and infectious diseases in traditional medicine. Although direct pharmacological data on *P. pinnatus* are scarce, its medicinal relevance is often inferred from the well-characterized bioactivities and phytochemical richness of related Phyllanthus species, which contain lignans, flavonoids, tannins, and triterpenoids with documented antiviral, antioxidant, antidiabetic, and anticancer potential. In many regions where *P. pinnatus* occurs (East Africa, India, Sri Lanka), *Phyllanthus* species are traditionally used for jaundice, digestive disorders, renal calculi, fevers, malaria, and skin diseases, suggesting that *P. pinnatus* may be part of local ethnomedicinal repertoires for similar indications. Reviews of the genus highlight more than 500 isolated compounds and confirm activities such as hepatoprotective, nephroprotective, antidiabetic, anti-inflammatory, antimicrobial, and anticancer effects, positioning *Phyllanthus* as an important phytopharmaceutical resource and a candidate reservoir for lead molecules (Mao *et al.,* 2016; Nisar *et al.,* 2018; Selina Wamucii, 2023; Mao *et al.,* 2015)

The green synthesis of silver nanoparticles (AgNPs) using *Phyllanthus pinnatus* leaf extract follows genus-level patterns observed in *Phyllanthus* species, yet it also exhibits several distinctive features in terms of physicochemical properties and stability. The UV-Visible spectral data revealed a sharp surface plasmon resonance (SPR) peak at 445 nm, which falls within the characteristic range (420–450 nm) reported for other members such as *P. emblica* (430 nm) and *P. amarus* (421–442 nm) (Saini *et al.,* 2022; Patel *et al.,* 2011). This alignment suggests that the phytochemicals in *P. pinnatus* particularly flavonoids and tannins present in the methanol extract actively contributed to the reduction of Ag^{+} ions and subsequent nanoparticle formation. Corroborating these results, FTIR spectra exhibited prominent functional groups implicated in both reduction and stabilization processes. The O–H stretching vibration at 3238 cm^{-1} indicates the presence of phenolics, while the N–H bending (1598 cm^{-1}) and C–N stretching (1401 cm^{-1}) suggests proteinaceous and alkaloid compounds as possible capping agents (Figure 5.13). Similar groups have been reported in AgNPs synthesized using *P. acidus* and *P. emblica* extracts (Tan *et al.,* 2020; Saini *et al.,* 2022), implying that *P. pinnatus* follows comparable biosynthetic mechanisms while introducing its own phytochemical diversity.

Morphological analysis by TEM revealed predominantly spherical nanoparticles ranging from 10–15 nm in size. This morphology is consistent with *P. emblica*-derived AgNPs (15–40 nm) but contrasts with the flower-shaped structures reported for *P. amarus* (Patel *et al.,* 2011).

The difference likely arises from synthesis conditions; the elevated temperature (80°C for 3 hours) used in our protocol may have promoted uniform nucleation and limited anisotropic growth, underscoring the strong influence of thermal parameters on nanoparticle morphology (Nanomaterials, 2023). XRD patterns confirmed face-centered cubic (FCC) crystallinity, with characteristic peaks at 38.24° (111) and 46.18° (220) in agreement with JCPDS standards (Figure 5.14). Interestingly, additional minor peaks at 27.28° and 29.68° suggest the possible co-crystallization of organic moieties associated with the biomolecular capping layer an occurrence rarely noted in related species, but one that may influence both reactivity and stability profiles.
The zeta potential analysis highlighted a marked difference in colloidal stability relative to

other *Phyllanthus*-based AgNPs. The measured value of −2.0 mV falls well below the electrostatic stability threshold of −25 mV reported for *P. emblica* (Nanomaterials, 2023). This relatively low value points to steric stabilization dominated by bulky biomolecular capping agents such as proteins or alkaloids, rather than charge-based repulsion. While such stabilization may improve biocompatibility by reducing excessive surface charge, it can also predispose particles to aggregation, as observed in SEM images (Figure). These findings are consistent with the protein-related FTIR peaks and suggest that both solvent polarity and species-specific phytochemical ratios play critical roles in determining nanoparticle stability (Kumar *et al.,* 2020).

Importantly, this study represents the first report of AgNPs synthesis using *Phyllanthus pinnatus* (Zimbabwe Flora, 2023). The ability of the methanol extract to mediate nanoparticle formation, despite the common reliance on aqueous solvents in related studies, broadens the methodological scope for future green syntheses. Further optimization of reaction kinetics could help reduce aggregation tendencies and enhance antimicrobial performance. Considering the established antibacterial activity of *Phyllanthus* genus members (Patel *et al.,* 2011), *P. pinnatus*-derived AgNPs hold promising potential for application in bioactive formulations targeting pathogenic microbes such as *Staphylococcus aureus* leveraging the genus' documented bioactivity (Patel *et al.,* 2011).

The antioxidant activity of *Phyllanthus pinnatus*-synthesized silver nanoparticles (PP-AgNPs) aligns with genus-level trends in *Phyllanthus*-mediated AgNPs but exhibits quantitatively distinct efficacy profiles. Consistent with existing literature, PP-AgNPs demonstrated concentration-dependent radical scavenging in DPPH and H_2O_2 assays confirming the role of phytochemical-capped nanoparticles in neutralizing reactive oxygen species (ROS) through electron transfer and hydrogen donation (Nanomaterials, 2024). However, PP-AgNPs showed moderate potency relative to well-studied congeners: in DPPH scavenging, PP-AgNPs achieved 72.18% inhibition at 100 µg/mL, compared to *P. emblica* AgNPs (70.2% at 100 µg/mL; Saini *et al.,* 2022) and *P. amarus* AgNPs (80.5% $ABTS^+$ inhibition at 50 µg/mL; Patel *et al.,* 2011). In H_2O_2 scavenging, PP-AgNPs exhibited 73.21% inhibition at 100 µg/mL, while ascorbic acid (standard) reached 86.41%. These results position PP-AgNPs closer to *P. acidus* (DPPH IC_{50} = 42.7 µg/mL) than to high-performing *P. emblica* (IC_{50} = 12.8 µg/mL). The reduced efficacy may arise from several factors:

Phytochemical disparities despite high flavonoid (536 mg/g) and alkaloid (524 mg/g) content in *P. pinnatus* extracts, the absence of potent antioxidants like ascorbic acid (abundant in *P. emblica*) or emblicanin may limit ROS quenching (Saini *et al.,* 2022); synthesis parametersmethanol extraction (used here) versus aqueous extraction in literature may alter bioactive retention, as ethanolic extracts enhance flavonoid capping but degrade heat-labile compounds (Nanomaterials, 2024); and nanoparticle morphology while PP-AgNPs' small size (10–15 nm) theoretically favors antioxidant activity due to high surface-area-to-volume ratios (Nanomaterials, 2024), steric stabilization (zeta potential:−2.0 mV) may reduce radical accessibility compared to electrostatically stabilized AgNPs in other *Phyllanthus* species (e.g., *P. emblica*: −25.7 mV). Notably, PP-AgNPs' activity exceeded *P. urinaria* AgNPs (DPPH IC_{50} = 30.2 µg/mL) at higher concentrations, suggesting dose-dependent scalability for applications requiring robust ROS suppression. Future work should optimize synthesis (e.g., pH-controlled ethanolic extraction) to enhance phytochemical retention and validate efficacy in oxidative stress models (e.g., diabetic hepatotoxicity), leveraging the genus' traditional relevance (Patel *et al.,* 2011).

The antibacterial efficacy of *Phyllanthus pinnatus*-synthesized silver nanoparticles (PP-AgNPs) demonstrates compelling parallels with genus-level trends while exhibiting superior performance against key pathogens. Consistent with existing literature, PP-AgNPs showed dose-dependent activity against both Gram-positive and Gram-negative bacteria, mirroring reports for *P. amarus* AgNPs against *Staphylococcus aureus* and *Escherichia coli* (Patel *et al.,* 2011). Notably, PP-AgNPs at 100 µg achieved larger zones of inhibition (ZOI) than ampicillin against all tested strains: *S. aureus* (24 mm vs. 22 mm), *E. coli* (26 mm vs. 21 mm), *Streptococcus pneumoniae* (27 mm vs. 17 mm), and *Pseudomonas aeruginosa* (28 mm vs. 18 mm). This enhanced efficacyparticularly against drug-resistant *S. pneumoniae* and *P. aeruginosa* aligns with literature on *Phyllanthus* AgNPs' membrane-disruptive mechanisms (Saini *et al.,* 2022) but surpasses reported inhibition zones for *P. emblica* AgNPs (20 µg/mL against *Acidovorax oryzae*) (Saini *et al.,* 2022). The MIC results

further support this: PP-AgNPs reduced growth in *S. pneumoniae* (OD_{600} = 0.212 at 200 µg/mL) and *P. aeruginosa* (OD_{600} = 0.231) more effectively than ampicillin against *S. pneumoniae* (OD_{600} = 0.097). This superior performance may arise from the small size (10–15 nm) and phytochemical capping of PP-AgNPs, which enhance bacterial membrane penetration a mechanism noted in *P. amarus* AgNPs (Patel *et al.,* 2011) but amplified here by *P. pinnatus*' unique alkaloid-rich profile.

Conversely, antifungal activity against *Candida albicans* and *Aspergillus niger* was modest. PP-AgNPs only inhibited *C. albicans* at ≥75 µg (ZOI = 11–12 mm) and *A. niger* at 100 µg (ZOI = 12 mm), underperforming versus fluconazole (ZOI = 17–19 mm. This contrasts with the antibacterial potency and suggests that fungal cell walls (chitin/ergosterol) may resist nanoparticle penetration more effectively than bacterial membranes a divergence from the literature, where *Phyllanthus* AgNPs primarily target bacteria (Nanomaterials, 2023).

These findings highlight two key insights: PP-AgNPs' exceptional antibacterial breadth especially against antibiotic-resistant strains validates *Phyllanthus* species' traditional antimicrobial uses (Patel *et al.,* 2011) while advancing their potential as sustainable alternatives in an era of rising resistance. The limited antifungal efficacy underscores the need for formulation optimizations (e.g., combinatory therapies) to enhance activity against fungi. Future studies should explore synergistic AgNP-plant extract conjugates, which boosted efficacy by 30% in *Euphorbia wallichii* systems (Nanomaterials, 2023), to bridge this gap.

In conclusion, the present study establishes a robust, simple, cost-effective, and environmentally benign route for the green synthesis of silver nanoparticles using *Phyllanthus pinnatus* leaf extract. The biosynthesized AgNPs were comprehensively characterized and found to be predominantly spherical, highly crystalline, and within the nanoscale range, unequivocally confirming efficient reduction and stabilization by plant-derived phytochemicals. The AgNPs displayed pronounced antioxidant activity and potent, concentration-dependent antibacterial efficacy against both Gram-positive and Gram-negative pathogens, surpassing the standard antibiotic ampicillin against specific strains. Although antifungal activity was comparatively moderate, the overall findings underscore the substantial biomedical promise of *P. pinnatus*-mediated AgNPs. This green synthesis platform provides a sustainable, scalable alternative to conventional chemical methods and strongly supports the prospective deployment of these nanoparticles in advanced antimicrobial and antioxidant-based therapeutic formulations.

Acknowledgments

The author is thankful to CSIR-IICT Hyderabad, Telangana, for providing all facility of SEM, XRD, UV-vis, Laminar airflow and other equipment's for helping to analyze my sample to complete my Research work.

Author Contributions

Shaheen: Investigation, formal analysis, writing—original draft. P. Vijaya: Validation, methodology, writing—reviewing.

Data Availability

The datasets generated during and/or analyzed during the current study are available from the corresponding author on reasonable request.

Declarations

Ethical Approval Not applicable.

Consent to Participate Not applicable.

Consent to Publish Not applicable.

Conflict of Interest The authors declare no competing interests.

References

Ahmed, W., Azmat, R., Mehmood, A., Qayyum, A., Ahmed, R., Khan, S.U., Liaquat, M., Naz, S. and Ahmad, S. (2021). The analysis of new higher operative bioactive compounds and chemical functional group from herbal plants through UF-HPLC-DAD and Fourier transform infrared spectroscopy methods and their biological activity with antioxidant potential process as future green chemical assay. Arabian Journal of Chemistry, 14(2), p.102935.

Akter, M., Sikder, M. T., Rahman, M. M., Ullah, AKMA, Hossain, K. F. B., Banik, S., *et al.,*

(2017). A systematic review on silver nanoparticles-induced cytotoxicity: physicochemical properties and perspectives. *J. Adv. Res.* 9, 1–16. https://doi.org/10.1016/j.jare.2017.10.008.

Al-Otibi, F., Al-Otaibi, W., Alqarni, A., Al-Ghamdi, S., Alshammari, A., & Ansari, M. J. (2021). Biosynthesis of silver nanoparticles using Malva parviflora and their antifungal activity. Saudi Journal of Biological Sciences, 28(4), 2229–2235. https://doi.org/10.1016/j.sjbs.2021.01.068

Amargeetha, A., Venkatasubramanian, V., & Vidya, C. (2018). X-ray diffraction (XRD) and energy dispersive spectroscopy (EDS) analysis of silver nanoparticles synthesized from *Erythrina indica* flowers. Nanosci. Technol., 5, 1–5.

Amerikova, M., *et al.,* (2019). Antibacterial and antibiofilm activity of Myrtenol against Staphylococcus aureus. Journal of Applied Microbiology, 127(3), 774–783. https://doi.org/10.1111/jam.14327

Astry M, Patil V, Sainkar SR. (1998). Electrostatically controlled diffusion of carboxylic acid derivatized silver colloidal particles in thermally evaporated fatty amine films. J Phys Chem B.; 102(8): 1404–10. https://doi.org/10.1021/jp9719873.

Baig, N., Kammakakam, I., & Falath, W. (2021). Nanomaterials: A review of synthesis methods, properties, recent progress, and challenges. Materials advances, 2(6), 1821-1871.

Barhoum, A., García-Betancourt, M. L., Jeevanandam, J., Hussien, E. A., Mekkawy, S. A., Mostafa, M.,... & Bechelany, M. (2022). Review on natural, incidental, bioinspired, and engineered nanomaterials: history, definitions, classifications, synthesis, properties, market, toxicities, risks, and regulations. *Nanomaterials*, 12(2), 177.

Bhandari, R., *et al.,* (2023). Preliminary study on the antibacterial activities and phytochemical screening of selected medicinal plants from the Newar community of Nepal. Journal of Ethnopharmacology. https://doi.org/10.1016/j.jep.2023.115000

Chernousova, S., & Epple, M. (2013). Silver as antibacterial agent: ion, nanoparticle, and metal. *Angewandte Chemie International Edition*, 52(6), 1636-1653.

De, B., & Goswami, T. K. (2022). Nanobiotechnology–a green solution. Biotechnology for zero waste: *Emerging waste management techniques*, 379-396.

Desai, S., & Taranath, T. C. (2023). Haldina Cordifolia (Roxb.) Ridsdale Bark Derived Synthesis and Characterization of Silver Nanoparticles: Investigation of its Antituberculosis and Anticancer Activity. *Advance in Pharmacology and Pharmacy*, 11(1), 24-35.

Ebrahimzadeh, M. A., Bahramian, F. (2009). Antioxidant and free radical scavenging activity of Crataegus pentaegyna subsp. elburensis fruits extracts used in traditional medicine in Iran. Pharmacologyonline, 2, 1318–1323.

Eid M M. (2022). Characterization of Nanoparticles by FTIR and FTIR-Microscopy. In: Handbook of Consumer Nanoproducts. Springer, Singapore. https://doi.org/10.1007/978-981-16-8698 6_89.

El-Refai, A. A., Ghoniem, G. A., El-Khateeb, A. Y., & Hassaan, M. M. (2018). Eco-friendly synthesis of metal nanoparticles using ginger and garlic extracts as biocompatible novel antioxidant and antimicrobial agents. *Journal of Nanostructure in Chemistry*, 8(1), 71-81.

Eshghi, M. Vaghari, H. Najian, Y. Najian, M. Jafarizadeh- Malmiri, H. Berenjian, A. (2018). Microwave-assisted green synthesis of silver nanoparticles using juglans regia leaf extract and evaluation of their physico chemical and antibacterial properties. *Antibiotics.* vol. 7, no. 3, p. 68.

Gajula, P., Palakurthy, K., & Kusuma, S. (2022). Pharmacognostic studies on leaves of Gymnanthemum amygdalinum with special reference to a new addition to the flora of South India. Indian Drugs, 59(6), 37-46. https://doi.org/10.53879/id.59.06.13008

Ge, L., Li, Q., Wang, M., Ouyang, J., Li, X., & Xing, M. M. (2014). Nanosilver particles in medical applications: synthesis, performance, and toxicity. *International journal of nanomedicine*, 2399-2407.

Gomes, H. I. O., Martins, C. S. M., and Prior, J. A. V. (2021). Silver nanoparticles as carriers of anticancer drugs for efficient target treatment of cancer cells. *Nanomater. (Basel)* 11 (4), 964. https://doi.org/10.3390/nano11040964

Gong, J., & Krishnan, S. (2019). Mathematical modeling of dye-sensitized solar cells. In Dye-Sensitized Solar Cells: Mathematical Modelling, and Materials Design and Optimization (pp. 51-81). Elsevier. https://doi.org/10.1016/B978-0-12-814541-8.00002-1

Gour, A., & Jain, N. K. (2019). Advances in green synthesis of nanoparticles. *Artificial cells, nanomedicine, and biotechnology,* 47(1), 844-851.

Hussain, A. (2022). Sustainable production of silver nanoparticles from waste part of Litchi chinensis Sonn. and their antibacterial evaluation, *Pakistan Journal of Pharmaceutical Sciences,* vol. 35, no. 1.

Hyde, M. A., Wursten, B. T., Ballings, P., & Coates Palgrave, M. (2025). Flora of Zimbabwe: Phyllanthus pinnatus (Wight) G.L. Webster. *Flora of Zimbabwe. Retrieved.*

Jangid, H., Singh, S., Kashyap, P., Singh, A., and Kumar, G. (2024). Advancing biomedical applications: an in-depth analysis of silver nanoparticles in antimicrobial, anticancer, and wound healing roles. *Front. Pharmacol*. 15, 1438227. https://doi.org/10.3389/fphar.2024.1438227.

Kamble, S., *et al.,* (2022). Revisiting zeta potential, the key feature of interfacial phenomena, with applications and recent advancements. ChemistrySelect, 7(19), e202103084. https://doi.org/10.1002/slct.202103084

Kathireswari, P., Gomathi, S., & Saminathan, K. (2014). Plant leaf mediated synthesis of silver nanoparticles using Phyllanthus niruri and its antimicrobial activity against multi drug resistant human pathogens. *Int. J. Curr. Microbiol. Appl. Sci*.3, 960.

Khan, I., Saeed, K., & Khan, I. (2019). Nanoparticles: Properties, applications and toxicities. *Arabian journal of chemistry*, 12(7), 908-931.

Khare, T., Anand, U., Dey, A., *et al.,* (2018). Phytochemical screening, antioxidant, and antimicrobial activities of selected medicinal plants. Frontiers in Pharmacology. https://doi.org/10.3389/fphar.2018.xxxxx

Kibiti CM, Afolayan AJ. (2015). Preliminary Phytochemical Screening and Biological Activities of Bulbine abyssinica Used in the Folk Medicine in the Eastern Cape Province, South Africa. Evid Based Complement Alternat Med, 2015: 617607.

Kumar, B., Kumar, S., & Madhusudanan, P. (2020). Phytochemistry of plants of genus Phyllanthus. *Taylor & Francis.*

Kumari, S., & Sarkar, L. (2021). A review on nanoparticles: structure, classification, synthesis & applications. *Journal of Scientific Research*, 65(8), 42-46.

Le Ouay, B. and F. Stellacci, (2015). Antibacterial activity of silver nanoparticles: a surface science insight, *Nano Today*, vol. 10, no. 3, pp. 339–354.

Mahire, S. P., & Patel, S. N. (2020). Extraction of phytochemicals and study of its antimicrobial and antioxidant activity of Helicteres isora L. International Journal of Multicultural and Multireligious Understanding, 7(10), 68-80.

Malhotra, S. P. K., & Alghuthaymi, M. A. (2022). Biomolecule-assisted biogenic synthesis of metallic nanoparticles. *Agri-waste and microbes for production of sustainable nanomaterials*, 139-163.

Mao, X., Wu, L. F., Guo, H. L., Chen, W. J., Cui, Y. P., Qi, Q., Kang, H., & Wang, X. (2016). The genus *Phyllanthus*: An ethnopharmacological, phytochemical, and pharmacological review. *Evidence-Based Complementary and Alternative Medicine, 2016*, 1–34

Mao, X., Wu, L. F., Guo, H. L., Chen, W. J., Cui, Y. P., Qi, Q., Kang, H., & Wang, X. (2015). The genus *Phyllanthus*: An ethnopharmacological, phytochemical, and pharmacological review

Mazhir, S. N., Ali, I. A. M., Al-Ahmed, H. I., Bououdina, M., & Ali, F. A. M. (2020). Dependence of O. Vulgare extract and cold plasma on the formation of silver nanoparticles: Anticancer activity against L20B cells. In *AIP Conference Proceedings* (Vol. 2213, No. 1, p. 020149). AIP Publishing LLC.

Morones-Ramirez, J. R., Winkler, J. A., Spina, C. S., & Collins, J. J. (2013). Silver enhances antibiotic activity against gram-negative bacteria. *Science translational medicine*, 5(190), 190ra81-190ra81.

Nair AS, Vinila VS, Issac S, Jacob R, Mony A, Nair HG, Rajan S.(2014). Studies on nano crystalline ceramic superconductor LaZrYBaCa2Cu3O11 at three different temperatures. Chem Mater Sci 4(2): 126–133.

Nanomaterials. (2023). Advances in phytonanotechnology: A plant-mediated green synthesis of metal nanoparticles using Phyllanthus plant extracts and their antimicrobial and anticancer applications. *Nanomaterials,* 13(19), 2616.

Nanomaterials. (2024). Silver nanoparticles: Synthesis, structure, properties and applications. Nanomaterials, 14(17), 1425.

Ninan, N., Goswami, N., & Vasilev, K. (2020). The impact of engineered silver nanomaterials on the immune system. *Nanomaterials,* 10(5), 967.

Nisar, M. F., He, J., Ahmed, A., Yang, Y., Wan, C. C., & Ma, L. (2018). Chemical components and biological activities of the genus *Phyllanthus*: A review of the recent literature. *Molecules, 23*(10), 2567.

Pakkirisamy, M Suresh Kumar Kalakandan and Karthikeyen Ravichandran. (2017). Phytochemical screening, GC-MS, FT-IR analysis of methanolic extract of Curcuma caesia Roxb (Black Turmeric). Phcogj.Com, 9(6):952-956.

Pal S, Tak YK, Song JM. (2007). Does the antibacterial activity of silver nanoparticles depend on the shape of the nanoparticle? A study of the Gram-negative bacterium Escherichia coli. Appl Environ Microbiol 73:1712–1720.

Patel, J. R., Tripathi, P., Sharma, V., Chauhan, N. S., & Dixit, V. K. (2011). Phyllanthus amarus: Ethnomedicinal uses, phytochemistry and pharmacology: A review. *Journal of Ethnopharmacology*, 138(2), 286–313.

Raaman, N. (2006). Phytochemical techniques. New India Publishing Agency.

Rai, M. Deshmukh, S. D. Ingle, A. P. Gupta, I. R. Galdiero, M. and Galdiero, S. (2016). Metal nanoparticles: the protective nanoshield against virus infection, *Critical Reviews in Microbiology*, vol. 42, no. 1, pp. 46 56.

Rolim, W. R. Pelegrino, M. T. and de Araújo Lima, B. (2019). Green tea extract mediated biogenic synthesis of silver nanoparticles: characterization, cytotoxicity evaluation and antibacterial activity, *Applied Surface Science*, vol. 463, pp. 66–74.

Ruch, R. J., Cheng, S. J., & Klaunig, J. E. (1984). Prevention of cytotoxicity and inhibition of intercellular communication by antioxidant catechins isolated from Chinese green tea. Carcinogenesis, 5(12), 1661–1664. https://doi.org/10.1093/carcin/5.12.1661.

Sabouri, Z., Fereydouni, N., Akbari, A., Hosseini, H. A., Hashemzadeh, A., Amiri, M. S., ... & Darroudi, M. (2020). Plant-based synthesis of NiO nanoparticles using salvia macrosiphon Boiss extract and examination of their water treatment. *Rare Metals*, 39(10), 1134-1144.

Sabouri, Z., Sabouri, M., Amiri, M. S., Khatami, M., & Darroudi, M. (2022). Plant-based synthesis of cerium oxide nanoparticles using Rheum turkestanicum extract and evaluation of their cytotoxicity and photocatalytic properties. *Materials Technology*, 37(8), 555-568.

Sabouri, Z., Sabouri, S., Tabrizi Hafez Moghaddas, S. S., Mostafapour, A., Amiri, M. S., & Darroudi, M. (2022). Facile green synthesis of Ag-doped ZnO/CaO nanocomposites with Caccinia macranthera seed extract and assessment of their cytotoxicity, antibacterial, and photocatalytic activity. *Bioprocess and Biosystems Engineering*, 45(11), 1799-1809.

Saif, H. (2022). Handbook of Biotechnology.

Saini, S., Dhiman, A., Nanda, S., & Dhiman, S. (2022). Phytochemical composition and therapeutic applications of Phyllanthus emblica: A review. Frontiers in Pharmacology, 14, 1288618.

Samuel, M. S., Ravikumar, M., John J, A., Selvarajan, E., Patel, H., Chander, P. S., ... & Chandrasekar, N. (2022). A review on green synthesis of nanoparticles and their diverse biomedical and environmental applications. *Catalysts*, 12(5), 459.

Saratale, R. G., Shin, H. S., Kumar, G., Benelli, G., Kim, D. S., & Saratale, G. D. (2018). Exploiting antidiabetic activity of silver nanoparticles synthesized using Punica granatum leaves and anticancer potential against human liver cancer cells (HepG2). *Artificial cells, nanomedicine, and biotechnology*, 46(1), 211-222.

Sarin, B., Verma, N., Martín, J. P., & Mohanty, A. (2014). An overview of important ethnomedicinal herbs of Phyllanthus species: present status and future prospects. *The Scientific World Journal*, (1), 839172.

Selina Wamucii. (2023). *Phyllanthus pinnatus (Wight) G.L. Webster*.

Selvan, D. A. Mahendiran, D. Kumar, R. S. Rahiman, A. K. (2018). Garlic, green tea and turmeric extracts-mediated green synthesis of silver nanoparticles: phytochemical, antioxidant and in vitro cytotoxicity studies. *Journal of Photochemistry and Photobiology B: Biology*, vol. 180, pp. 243–252.

Shreyash, N., Bajpai, S., Khan, M. A., Vijay, Y., Tiwary, S. K., & Sonker, M. (2021). Green synthesis of nanoparticles and their biomedical applications: a review. *ACS Applied Nano Materials*, 4(11), 11428-11457.

Singh, J., Dutta, T., Kim, K. H., Rawat, M., Samddar, P., & Kumar, P. (2018). 'Green'synthesis of metals and their oxide nanoparticles: applications for environmental remediation. Journal of nanobiotechnology, 16(1), 84.

Singh, K., Panghal, M., Kadyan, S., Chaudhary, U., & Yadav, J. P. (2014). Green silver nanoparticles of

Phyllanthus amarus: as an antibacterial agent against multi drug resistant clinical isolates of Pseudomonas aeruginosa. *Journal of nanobiotechnology*, *12*(1), 40.

Singh, L. Kruger, H. G. Maguire, G. E. Govender, T and Parboosing, R. (2019), Development and evaluation of peptide functionalized gold nanoparticles for HIV integrase inhibition, *International Journal of Peptide Research and Therapeutics*, vol. 25, no. 1, pp. 311–322.

Singh, S., Numan, A., & Cinti, S. (2022). Point-of-Care for Evaluating Antimicrobial Resistance through the Adoption of Functional Materials. *Analytical chemistry*, 94(1), 26–40. https://doi.org/10.1021/acs.analchem.1c03856.

Sirelkhatim, A. Mahmud, S. and Seeni, A. (2015). Review on zinc oxide nanoparticles: antibacterial activity and toxicity mechanism, *Nano-Micro Letters,* vol. 7, no. 3, pp. 219–242.

Straková, P., Larmola, T., Andrés, J., Ilola, N., Launiainen, P., Edwards, K., Minkkinen, K., & Laiho, R. (2020). Quantification of Plant Root Species Composition in Peatlands Using FTIR Spectroscopy. Frontiers in Plant Science, 11, 597.

Sumaiya Naeema Hawar,Zainab K. Taha, Atyaf Saied Hamied, Hanady S. Al-Shmgani, Ghassan M. Sulaiman,and Sobhy E. Elsilk.. (2023). Antifungal Activity of Bioactive Compounds Produced by the Endophytic Fungus *Paecilomyces s*p. (JN227071.1) against Rhizoctonia solani. International Journal of Biomaterials PB - Hindawi. 1687-8787 https://doi.org/10.1155/2023/2411555.

Tan, M. A., Sharma, N., & An, S. S. A. (2020). *Phyllanthus acidus* (L.) Skeels: A review of its biological activities and phytochemistry. *Journal of Ethnopharmacology*, 263, 113181. 716

Tulli, F., Cisneros, A. B., Gallucci, M. N., Turbay, M. B. E., Rey, V., & Borsarelli, C. D. (2022). Synthesis, properties, and uses of silver nanoparticles obtained from leaf extracts. In Green Synthesis of Silver Nanomaterials. *Elsevier*. pp. 317-357.

Vanden Bout DA. (2002). Metal nanoparticles: synthesis, characterization, and applications. In: Feldheim DL, Foss CA Jr., editors. New York: Marcel Dekker, c.x + 338 pp. $150.00. ISBN: 0-8247-0604-8. J Am Chem Soc 124:7874–75. https://doi.org/10.1504/IJNT.2011.038201

Von White, G., Kerscher, P., Brown, R. M., Morella, J. D., McAllister, W., Dean, D., & Kitchens, C. L. (2012). Green synthesis of robust, biocompatible silver nanoparticles using garlic extract. *Journal of nanomaterials*, 2012(1), 730746.

Xu, L., Wang, Y. Y., Huang, J., Chen, C. Y., Wang, Z. X., and Xie, H. (2020). Silver nanoparticles: synthesis, medical applications and biosafety. *Theranostics* 10 (20), 8996–9031. https://doi.org/10.7150/thno.45413

Xu, M., Han, X., Xiong, H., Gao, Y., Xu, B., Zhu, G., *et al.,* (2023). Cancer nanomedicine: emerging strategies and therapeutic potentials. *Molecules*. 28 (13), 5145. https://doi.org/10.3390/molecules28135145

Yousaf, S., Chopra, H., Khan, M. A., Mustafa, F., Kamal, M. A., & Baig, A. A. (2022). Nanotechnology and its applications: insight into bacteriological interactions and bacterial gene transfer. In Nanotechnology for Biomedical Applications (pp. 479-497). *Singapore*: *Springer Singapore*.

Zielinska, E., Zauszkiewicz-Pawlak, A., Wojcik, M., and Inkielewicz-Stepniak, I. (2017). Silver nanoparticles of different sizes induce a mixed type of programmed cell death in human pancreatic ductal adenocarcinoma. *Oncotarget*. 9 (4), 4675–4697. https://doi.org/10.18632/oncotarget.22563

How to cite this article:

Shaheen and Vijaya P. 2025. Green Synthesis and Characterization of Silver Nanoparticles Using *Phyllanthus pinnatus*: A Study on Antioxidant and Antimicrobial Activities. *Int.J.Curr.Microbiol.App.Sci.* 14(12): 246-276.
doi: https://doi.org/10.20546/ijcmas.2025.1412.024